HEAT TRANSFER ANALYSIS OF THERMOSIPHONS AND U-TUBE GROUND SOURCE HEAT PUMPS

by

Joshua Nakaoka

A thesis submitted to the faculty of
The University of Utah
in partial fulfillment of the requirements for the degree of

Master of Science

Department of Mechanical Engineering

The University of Utah

December 2012

The University of Utah Graduate School

STATEMENT OF THESIS APPROVAL

The thesis of **Joshua Nakaoka**

has been approved by the following supervisory committee members:

Kent Udell	, Chair	**10/05/2012** Date Approved
Timothy Ameel	, Member	**10/08/2012** Date Approved
Kuan Chen	, Member	**10/08/2012** Date Approved

and by **Timothy Ameel** , Chair of the Department of **Mechanical Engineering**

and by Charles A. Wight, Dean of The Graduate School.

ABSTRACT

Ground source thermal energy transport systems have the potential to improve the efficiency of space heating.

Two such systems, a thermosiphon and a vertical U-tube system, were installed in a housing unit in Park City, Utah with the aim of assessing performance. From temperature measurements, the heating Coefficient of Performance (COP) for the U-tube system was determined to be around 3. When taking into consideration only space heating, because of the poor performance of the U-tube system and the relatively inexpensive cost of natural gas, the high installation cost of this particular U-tube GSHP will not be recouped in energy cost savings. COP was not used to assess the thermosiphon, but the heat transfer rate per unit length associated with the thermosiphon was found to be approximately 2.3 times greater than that of the U-tube system.

Transient temperature measurements led to the development of a conceptual heat transfer model that described the convective heat transfer between flowing groundwater and the thermal grout sealing each piping network. Using this model, a method was developed to infer the convective heat transfer coefficient of each system directly from temperature measurements along the outside of each piping network without directly measuring groundwater velocity. From this method, the heat transfer coefficient for the U-tube was accurately found to be between 8 and 14.4 W/m^2-K.

TABLE OF CONTENTS

ABSTRACT iii
LIST OF TABLES v
LIST OF FIGURES vi
NOMENCLATURE vii
ACKNOWLEDGMENTS ix
1 INTRODUCTION 1
1.1 Background 2
1.2 Vertical U-tube GSHPs 5
1.3 Thermosiphons 8
2 LITERATURE REVIEW 11
2.1 U-Tube GSHP Literature 11
2.2 Thermosiphon Literature 14
3 EXPERIMENTAL SETUP 16
4 RESULTS 21
4.1 Ground Source vs. Air Source 21
4.2 Performance 24
4.3 Heat Transfer Analysis 33
5 CONCLUSIONS 52
5.1 Recommendations 54
REFERENCES 56

LIST OF TABLES

4.1: COP Results. 27
4.2: Values of λ_1 for various Biot numbers. $\beta = R_i/R_o$. 40

LIST OF FIGURES

1.1: U-tube Ground Loop 6
1.2: The U-tube Operating Principle 7
1.3: Thermosiphon Operating Principle 10
3.1: Experimental Setup 20
4.1: Daily Average Winter Temperatures. 22
4.2: Relationship between Ambient Temperature, Heating Load, and Fluid Inlet Temperature 23
4.3: Unit 10 U-tube COP from November 24, 2010 to December 22, 2010 25
4.4: Unit 10 U-tube COP from February 14, 2011 to March 4, 2011. 26
4.5: Unit 10 U-tube COP from December 30, 2011 to January 13, 2012 26
4.6: Unit 11 U-tube COP from February 15, 2011 to March 4, 2011 27
4.7: Heat Pump Fluid Inlet Temperatures 29
4.8: Impact of Inline Pump on Performance 30
4.9: Heat Transfer per Unit Length 33
4.10: Thermosiphon Transients 34
4.11: U-tube Transients 34
4.12: Conceptual Heat Transfer Model. 36
4.13: First Eigenvalue as a Function of the Biot Number 41
4.14: Natural Logarithm of Scaled Temperature vs Time for the Unit 10 Thermosiphon on November 22, 2010 43
4.15: Natural Logarithm of Scaled Temperature vs Time for Unit 10 U-tube on November 22, 2010 45
4.16: Natural Logarithm of Scaled Temperature vs Time for Unit 10 U-tube on February 23, 2012 46
4.17: Natural Logarithm of Scaled Temperature vs Time for Unit 11 U-tube on February 23, 2012 46
4.18: Subterranean Temperature Profile. 50

NOMENCLATURE

COP	Coefficient of Performance
$COP_{HP,rev}$	Coefficient of Performance of a reversible Carnot heat pump
T_H	temperature of the high-temperature reservoir
T_L	temperature of the low-temperature reservoir
QH	heat transferred to the high-temperature reservoir
W_{net}	net work input
$\dot{W_{net}}$	rate of net work input
$\dot{Q}_L$	rate of heat transferred from the low-temperature reservoir
c_p	specific heat
ρ	density
$\dot{V}$	volume flow rate
ΔT	temperature difference between the glycol solution exiting and entering the heat pump
$\frac{\partial T}{\partial r}$	change in temperature with respect to radial position
r	radial position
T	temperature
t	time
q'	heat transfer per unit length from the inside surface of the grout
k_g	thermal conductivity of the thermal grout
R_i	inside grout radius
R_o	outside grout radius
h	outside heat transfer coefficient
T_∞	ambient temperature of the groundwater
$T(r)$	steady-state temperature distribution
Bi	Biot number

$F(r)$	steady state temperature distribution
$T(r,t)$	transient temperature distribution
C_m	Constants in transient solution
λ_m	eigenvalues
$R(\lambda_m, r)$	solution of subproblem within transient solution
β	ratio of inside to outside grout radii
$J_o(\lambda_m)$	Bessel function of the first kind of order zero
$Y_1(\lambda_m)$	Bessel function of the second kind of order one
$Y_o(\lambda_m)$	Bessel function of the second kind of order zero
$J_1(\lambda_m)$	Bessel function of the first kind of order one
Fo	Fourier number
α_g	thermal diffusivity of the grout
λ_1	first eigenvalue
$T(0)$	initial temperature
T_f	final steady state temperature
n	slope of linear slope-fit
Nu_D	Nusselt Number
k_s	thermal conductivity of the local permeable soil
D	the outside diameter of the grout
V	groundwater velocity
K	hydraulic conductivity
$\frac{dh}{dl}$	hydraulic gradient
k	soil permeability
g	acceleration due to gravity
μ	dynamic viscosity
Re_D	Reynolds number
Pr	Prandtl number
Pe_D	Peclet number
α_s	thermal diffusivity of the soil
k_s	thermal conductivity of the soil

ACKNOWLEDGMENTS

I would like to thank my adviser, Dr. Kent S. Udell, for his continued support and guidance throughout this project. When I was faced with messy mathematical equations, Dr. Udell simplified the problem so that I could understand the practical implications behind the math.

I wish to thank the other thesis committee members Dr. Ameel and Dr. Chen for reviewing my thesis and providing valuable feedback.

I would like to acknowledge Christopher Workman for putting in long hours and dealing with the frustrations of overseeing the implementation of the experimental setup for this thesis. Because of Chris, I was able to focus on data analysis and interpretation.

I would also like to thank Bidzina Kekalia for helping me to understand my role when I first started working for Dr. Udell. He helped me understand what to expect in graduate school and how to stay motivated through any situation.

CHAPTER 1

INTRODUCTION

In 2010, buildings accounted for more than 40% of the total primary energy consumption in the United States with much of this energy being used for space heating. This is especially true in the residential sector where space heating accounted for 45% of site energy consumption. According to the United States Department of Energy, "Space heating and cooling—which combined accounts for 54% of site energy consumption and 43% of primary energy consumption—drives residential energy demand [1]." With much of this energy demand being met by burning fossil fuels such as natural gas and coal, improved efficiency in residential heating can lower energy costs, improve air quality, and reduce fossil fuel emissions.

One way to increase space heating efficiency is to utilize the ground as a source of thermal energy. During the heating season, the ground is warmer than the ambient air; accordingly, ground source thermal energy transport systems have the potential to be more efficient than conventional air source heat pumps (ASHPs). Several studies indicate that this is the case. They claim that the predominant ground source heat transfer system, the U-tube ground source heat pump (GSHP), is more efficient and more economical than both ASHPs and natural gas furnaces. This study reexamined these claims by assessing the heating performance and economic viability of a vertical U-tube GSHP.

Another system, the thermosiphon, was also analyzed in this study. The thermosiphon has not been used extensively for ground source heat transfer, but it is theoretically capable of rapid heat transfer from one end of the system to the other. For this reason, both systems were installed in a housing unit in Park City, Utah, and the heat transfer rates for both the thermosiphon and the U-tube system were compared.

From observed temperature transients, it was hypothesized that flowing groundwater would increase heat transfer to the U-tube system and the thermosiphon. In order to determine the convective heat transfer coefficient, the velocity of the groundwater had to be determined. However, it is very difficult to directly measure groundwater velocities. This led to the development of a method for inferring the heat transfer coefficient using only temperature measurements. Thus, in addition to assessing the heating performance of each system, this work also developed a method for inferring the heat transfer coefficient without directly measuring the velocity of groundwater.

1.1 Background

Geothermal energy systems such as geysers, hot springs, and fumaroles (steam vents) have been used since ancient times for hot water heating and even space heating to a limited extent. Starting in the 1920s, the heating potential of these geothermal energy sources began to be realized on a large scale. By the 1960s, steam from these phenomena was used for turbine power generation. Since then, this type of geothermal energy has been used to successfully meet the energy needs of entire communities, but because these sources are associated with localized tectonic plate boundaries, they are “limited in their location and ultimate potential for supplying electricity,” [2].

These localized phenomena are not the only geothermal systems that can be effectively utilized as an energy source. In fact, the ground just below the Earth's surface is available almost anywhere and remains a mostly untapped energy source. Soil is a relatively poor conductor. As such, below a depth of approximately 5 meters, ground temperatures remain fairly constant and heat loss to the ambient air is greatly reduced. This creates a thermal lag. For example, if the ambient air is at a certain temperature, the soil at a depth of 20 feet will not reach this temperature immediately. It will take even longer for the soil at a depth of 30 feet to reach this temperature. This lag will increase with increasing depth. Because of this lag, temperatures below the surface tend to be milder than air temperatures. With soil having a large thermal capacity and being available almost anywhere, these milder temperatures can be utilized to meet the heating and cooling needs of even large buildings. All these properties combine to make the ground a very attractive alternative energy source with a great untapped energy potential [3].

Some systems such as GSHPs can take advantage of this energy potential to improve residential heating efficiencies. During the summer, the ground is cooler than the ambient air, and during the winter, the ground is warmer than the ambient air. Taking advantage of this dynamic, these systems transfer heat to the ground during the cooling season and from the ground during the heating season. This heat transfer usually occurs as a result of conduction between the soil and a subterranean heat exchanger. In locations with high groundwater flow, heat transfer can occur as a result of convection. In either case, heat is transferred from the ground during the heating season and to the ground during the cooling season [3].

Additional thermal energy potential can be gleaned from these systems in the form of seasonal energy storage. Using the ground as a heat source during the winter takes heat out of the soil. This stored “cold” can then be utilized during the summer as a heat sink for space cooling applications. During the summer, heat is again transferred to the ground. This stored heat can then be utilized during the winter as a heat source for space heating applications. In this way, both heating and cooling efficiencies can be improved [4].

By utilizing the ground as a heat sink during the summer and as a heat source during the winter, GSHPs have been found to be more efficient than other systems particularly air source heat pumps (ASHPs). For ASHPs, air is the heat source for heating and the heat sink for cooling. While this is relatively effective in most cases, using air as a heat source/sink requires additional energy input to adequately warm or cool a building. In cold heating seasons, as predicted by Carnot cycle analysis, the high temperature difference between the outside air and the heat pump refrigerant can drop the heat pump Coefficient of Performance (COP) considerably. In the same way, in hot cooling seasons, the Energy Efficiency Ratio (EER) of an ASHP can decrease significantly as the temperature of the condenser increases. COP rates the heating performance of a heat pump, and EER rates cooling performance. As a result of the milder temperatures of the ground in comparison to the ambient air, GSHPs have been found to be significantly more efficient than ASHPs. Compared to a typical ASHP, a GSHP can reduce green house gas emissions by 66% and can decrease energy consumption by 44%. The maintenance cost for a GSHP is half the cost of an ASHP, and the operating cost for a GSHP is a quarter of the cost of an ASHP [5].

The specific method of ground source heat transfer depends on the available land area and the geological conditions of the soil. The most common ground source system is the closed loop GSHP [6]. It can be implemented in either a horizontal or a vertical configuration. The horizontal method is cheaper as it only involves the digging of shallow trenches; whereas, the vertical configuration involves the drilling of deep boreholes. On the other hand, the horizontal method requires a large land area to effectively heat a building. In many instances, especially for residential housing units, large land area is not possible. As such, where geological conditions allow for deep boreholes, the vertical U-tube configuration is preferred. Another newer innovation, the thermosiphon, is associated with high latent heat capture and can also be employed in a vertical configuration. For these reasons, this study will focus on the heat transfer of thermosiphons and vertical U-tube GSHPs.

1.2 Vertical U-tube GSHPs

Both thermosiphons and U-tube GSHPs absorb heat from the ground and transfer that heat to a refrigerant in a heat pump system, but each performs this task in a different way. A vertical U-tube GSHP is an active heat exchanger in that an inline pump pulls a working fluid through a series of pipes in order to facilitate heat transfer with the ground. This subterranean heat exchanger is a closed U-shaped network of high-density polyethylene (HDPE) piping situated in a deep borehole. Boreholes can be 75 to 500 feet deep and 3 to 6 inches wide depending on apparent soil conductivity, location, and geology. The nominal diameter of the pipe is usually about 1 inch. Thermal grout often surrounds the pipe allowing for a better thermal connection with the soil [7]. A working

fluid, typically a mixture of water and antifreeze (ethylene glycol, propylene glycol, or methanol) is pumped through the U-tube ground loop. During winter, the fluid is at a lower temperature than the ground. As it flows through the U-tube network, the working fluid picks up heat from the ground. The fluid is then pumped up to the surface where it supplies heat to a heat pump. This thermal energy is then used to heat the building. The fluid flows back into the U-tube piping, and the cycle repeats [8]. Figure 1.1 shows the subterranean heat exchanger ground loop of a vertical U-tube GSHP system. The operating principal of the U-tube system is shown in Figure 1.2.

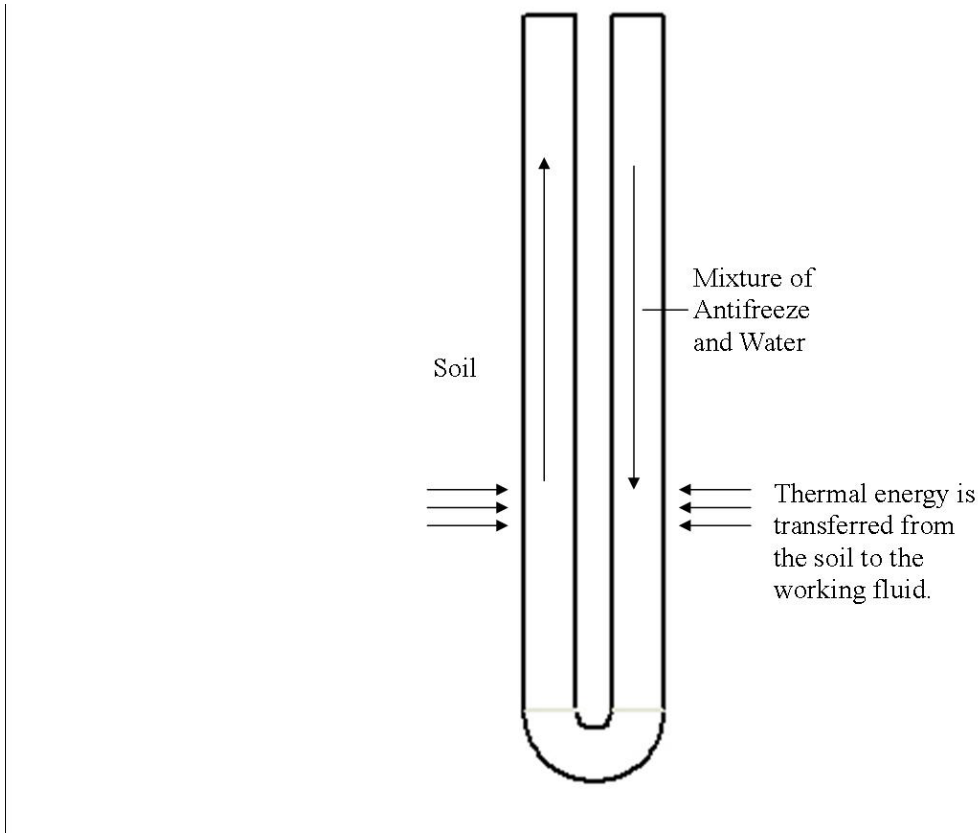

Figure 1.1: U-tube Ground Loop. To heat a typical home, three ground loops are usually necessary. Each of these loops runs 75 to 500 feet deep.

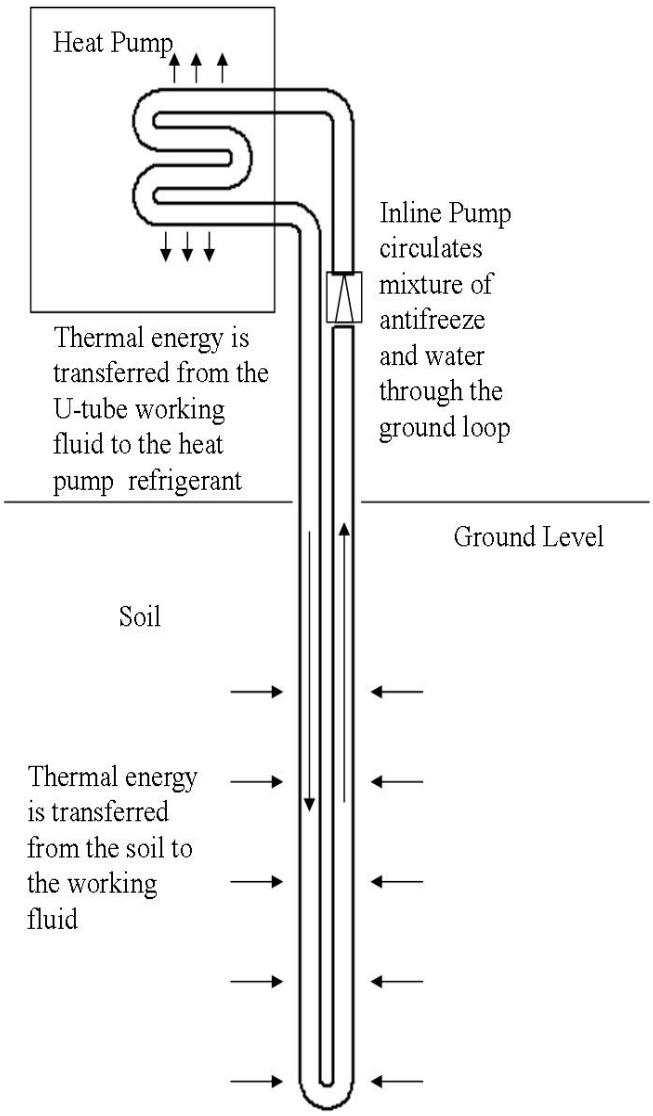

Figure 1.2: The U-tube Operating Principle. The U-tube extracts heat from the ground by using a long pipe as a heat exchanger in the ground. An antifreeze water mixture is pumped through the U-tube. Because the working fluid is cooler than the ground, it extracts heat from the warmer ground and exits the U-tube at a warmer temperature than when it entered. It then exchanges this heat with the heat pump refrigerant. To provide space heating, the heat pump operates on a refrigeration cycle.

A vertical U-tube GSHP can also be used for space cooling. In the summer, the working fluid is warmer than the surrounding ground and will lose heat to the ground. It is then pumped to the surface where it receives heat from a heat pump. Once the fluid has gained heat, it will return to the U-tube piping network and the process will repeat.

1.3 Thermosiphons

Unlike U-tube systems, thermosiphons rely on a passive method of fluid circulation, namely natural convection. The system relies on the evaporation and condensation of a working fluid to enable heat transfer. As such, thermosiphons do not require inline pumps. This idea was first developed and patented by R.S. Gaugler in 1942. In 1962, the concept took practical shape in G.M. Grover's invention of the heat pipe. The heat pipe is an evacuated copper or aluminum pipe containing a working fluid. It is designed to rapidly transfer heat from one end of the pipe to the other. Heat is applied to one side of the pipe, vaporizing the working fluid on that side of the pipe. This action creates a pressure gradient that transports the vapor to the other side of the pipe. At this end of the pipe, the vapor transfers its heat and condenses. The capillary action of wicking materials returns the condensed liquid to the other side of the pipe, and the process repeats [9].

There are several characteristics of heat pipes that make them appealing for commercial application. Originally designed for space applications, heat pipes do not need gravity to operate. They are lightweight and easily maintained. Heat pipes have high heat transfer rates and high latent heat capture capabilities allowing them to take advantage of small temperature differences (even single digit differences). Because of these properties, the heat pipe has been used in many applications including spacecraft thermal management, solar water heating, industrial heat exchange, and electronic cooling.

The thermosiphon was developed as a variation of the heat pipe. Instead of using the capillary action of wicking materials to return the working fluid to the hot side,

thermosiphons depend on gravity. Also, instead of employing pressure gradients to transport the fluid to the cold side, thermosiphons rely on the fact that a vapor will rise in the presence of a more dense liquid. For ground source heat transfer, an evacuated pipe is placed in a borehole and sealed with thermal grout much like the U-tube piping network. The pipe is then charged with a working fluid, usually a refrigerant. In an evacuated pipe with an elevation gradient, the working fluid will flow from the high point to the low point. The working fluid collects at the bottom of the pipe. Heat is transferred from the ground to the fluid, vaporizing the fluid. The vapor, being less dense than the surrounding fluid, will rise towards the top of the thermosiphon. At the top of the thermosiphon, the fluid condenses as it supplies heat to a space. The refrigerant drips down the walls of the pipe, and the process repeats. A diagram illustrating this process is shown in Figure 1.3.

Unlike the U-tube system, this passive thermosiphon configuration will not work for space cooling, but space cooling is possible in a reversible or pump-assisted thermosiphon configuration. In this configuration, at the top of the thermosiphon, the working fluid absorbs heat from the building. The fluid vaporizes, and pressure gradients allow the vapor to sink to the bottom of the thermosiphon. Heat is transferred from the working fluid to the ground. As a result of this heat exchange, the vapor condenses and is then pumped back to the top of the thermosiphon where the process repeats.

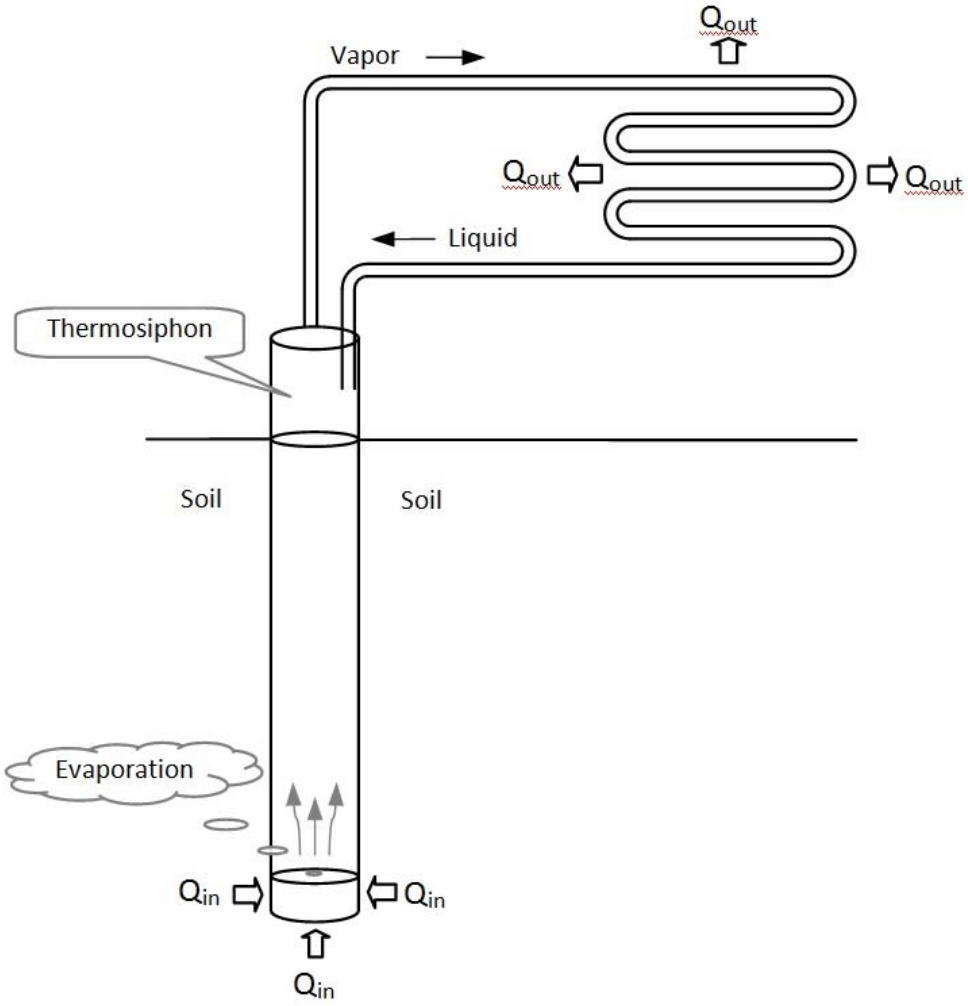

Figure 1.3: Thermosiphon Operating Principle. Gravity causes the liquid refrigerant to drip towards the bottom of the thermosiphon. The working fluid collects at the bottom of the pipe and vaporizes as it absorbs heat from the ground. The vapor, being less dense than the surrounding fluid, rises to the top of the thermosiphon where it supplies heat to a space. In losing thermal energy, the refrigerant condenses and the cycle repeats [4].

CHAPTER 2

LITERATURE REVIEW

Ground source heat exchange is not a new idea; the first patent awarded for the first GSHP was developed in the 1940s [10]. Since then, the GSHP has become the most common ground source heat transfer system with more than 1.1 million GSHP systems installed worldwide [6]. The GSHP is a relatively more mature technology than the thermosiphon. As such, there have been numerous studies on U-tube GSHPs, but very few studies have been conducted on utilizing thermosiphons for ground source heat exchange.

2.1 U-Tube GSHP Literature

Several vertical U-tube GSHP projects have been undertaken recently. The highest energy savings have been associated with large scale commercial or industrial installations. For example, in 2006, Lipscomb University completed construction of a U-tube system consisting of 140 boreholes each drilled to a depth of 300 feet. This system is responsible for the heating and cooling requirements of the 77,000 square foot Ezell center. The system cost $1.2 million to install. With $70,000 to $90,000 in annual energy savings and low maintenance costs, the system paid itself off in 16 months [11].

Another study looked at GSHP performance on a broader scale. This study was conducted in 1994 and included a performance review of 256 GSHP case studies. In this review, the performance of GSHPs was compared to typical ASHPs. It was found that for residential systems, annual energy savings ranged from 31% to 71%, and annual cost savings ranged from 18% to 54%. For school buildings, annual energy savings ranged from 51% to 76%, and annual cost savings ranged from 13% to 58%. For commercial buildings, annual energy savings ranged from 40% to 72%, and annual cost savings ranged from 31% to 56%. It was found that the average simple payback for residential buildings was 7 years. The average simple payback for commercial buildings was less than 3 years. This review also found that the COP of GSHPs ranged from 3 to 5 and the EER ranged from 20 to 12 [12].

Because the U-tube GSHP is a fairly established technology, current research is geared towards improving the GSHP system. One problem is the long term effects GSHPs have on ground temperatures. If the heating season is significantly shorter than the cooling season, more heat will be put into the ground than is taken out. Eventually, the ground will no longer act as an efficient heat sink, and the system will no longer be viable for space cooling. The temperature change around the system should be kept small so as to avoid performance reductions. To limit the temperature change around the boreholes, the ground loops must be appropriately sized. The same is true to a lesser extent if the heating season is longer than the cooling season. In both situations, the system size must be optimized so as to maintain steady ground source heat transfer. In 1987, Per Eskilon of the University of Lund in Sweden developed a model to accurately predict the response of a ground loop heat exchanger to continuously changing building

loads [13]. In 2000, a team of researchers from Oklahoma State University built upon and improved Eskilon's model. Using simulations and experimental data, they developed a procedure for designing and sizing a vertical U-tube GSHP so that it will remain viable over the course of its operating life [14].

The effect of groundwater flow must also be taken into account when designing and sizing a vertical U-tube GSHP. The enhanced convective heat transfer rates associated with groundwater have made locations with high groundwater velocities attractive locations for GSHPs. However, there has been a problem correctly sizing GSHP systems in these locales. One of the key parameters in sizing ground loops is the apparent thermal conductivity of the soil. It has been found that thermal conductivity tests overestimate the apparent thermal conductivity of the soil in locations with moderate to high groundwater flow rates. In these cases, the ground loops are undersized resulting in poor system performance. Currently, research is being done to create an improved sizing model that takes into account the flow of groundwater [15].

Other studies have investigated the thermal performance of GSHPs. Recently, the thermal performance of double U-pipes was analyzed and compared with single U-pipes. In a single U-pipe configuration, a single ground loop is placed in each borehole. They are most common in North America and Northern Europe. In a double U-pipe configuration, two ground loops are placed in the same borehole. They are most common in Central Europe. Simulations were used to compare the heat transfer rates associated with each of these configurations. The thermal resistance of the single U-pipe was determined to be 0.11 Kelvin-meters/Watt (K-m/W). The thermal resistance of the double U-pipe was determined to be 0.06 K-m/W [16].

2.2 Thermosiphon Literature

Although not to the same extent as GSHPs, thermosiphons have been used successfully in several applications. Thermosiphons have often been used for solar heat transfer applications especially for solar water heating. In a solar water heater application, a sloped evacuated glass pipe is filled with a working fluid. As a result of gravity, the working fluid collects at the bottom of the pipe. The sun supplies solar thermal energy to the bottom of the pipe vaporizing the working fluid. The now less dense vapor rises to the top of the pipe where it exchanges heat with a water tank. As a result of this heat exchange, the vapor condenses and drips down the side of the pipe and the cycle repeats [17].

This same principle has been applied to ground source heat transfer as well. A large scale thermosiphon array was installed in 1969 as part of the Trans-Alaskan pipeline. The pipeline supports were built mostly above permafrost. To keep the supports stable, the permafrost had to be kept frozen. To do this, thermosiphons were placed inside the supports to take heat out of the ground. More than 124,300 thermosiphons were installed as part of this project [18]. In 2000, this project was reviewed, and it was found that several of the thermosiphons had experienced a reduction in heat transfer performance due to an accumulation of noncondensable gases at the top of the thermosiphons. This phenomenon, known as cold topping, was a result of corrosion or chemical dissociation of the working fluid, anhydrous ammonia [19].

Thermosiphons have also been implemented successfully in space heating applications. In Belarus, thermosiphons have been used to keep greenhouse temperatures above freezing [20]. In Northern Austria, a corrugated steel thermosiphon was installed to

heat a residential building. The working fluid of this particular thermosiphon was carbon dioxide (CO2). The thermosiphon was placed in a borehole that had been drilled down to a depth of 100 meters. An inline pump was installed for increased fluid circulation. During the winter of 2006-2007, the thermosiphon was able to successfully heat the home with an average COP of 4.1 [21].

Some experimental work with reversible thermosiphons has also been conducted at the University of Utah. In 2009, a COMSOL computer simulation of a thermosiphon array indicated that compared to a U-tube GSHP, the thermosiphon design would increase heat transfer by 250%. This finding indicates that thermosiphon boreholes need not be as deep as U-tube boreholes. If a U-tube system requires a borehole of 250 feet, the thermosiphon would only require a 100 foot borehole. To verify this result, a small scale array of seven thermosiphon prototypes was installed at depths of 10 feet. As expected, temperature readings showed that thermal energy was successfully being transferred from the ground to the thermosiphon system [4, 22].

CHAPTER 3

EXPERIMENTAL SETUP

Based on the literature, system performance, economics, and subterranean heat transfer are very important considerations when evaluating ground source thermal energy transport systems. An experimental setup was implemented with these considerations in mind. A thermosiphon and a three loop U-tube GSHP system were both installed in a housing unit in Park City, Utah. The housing unit of concern, unit 10, is part of Snow Creek Cottages, a recently constructed sustainable housing development. This location has a relatively high apparent soil conductivity (3.79 Watts/meter-Kelvin [W/m-K]) compared to the average conductivity in the rest of the Central Utah Valley (1.73 Watts/meter-Kelvin [W/m-K]). The higher relative thermal conductivity increased heat transfer rates to the piping networks and allowed for shallower than normal boreholes; the boreholes for both systems were drilled down to depths of only 90 feet. The piping networks for each system were placed in the boreholes and sealed with Cetco geothermal grout (thermal conductivity of approximately 1.85 W/m-K). The thermosiphon was composed of galvanized steel, and the U-tube piping network was composed of HDPE piping. The systems were installed while the Snow Creek Cottage housing units were still under construction.

A unique configuration was employed to allow both the thermosiphon and the U-tube piping network to supply thermal energy to a heat pump located in the attic of housing unit 10. For both the thermosiphon and the U-tube piping network to supply thermal energy to the heat pump, it was necessary for both systems to use the same working fluid. The working fluid for the U-tube system was an ethylene glycol water mixture (30% ethylene glycol, 70% water), but the working fluid for the thermosiphon was R-134a. To solve this problem, a shell-and-tube heat exchanger was installed to transfer heat from the R-134a in the thermosiphon to a glycol mixture in an adjacent pipe.

To collect data on each system independently, only one system was allowed to supply thermal energy to the heat pump at any given time. The systems were installed in parallel with a single pipe carrying ethylene glycol from either the thermosiphon system or the U-tube system depending on the configuration of three-way diverting ball valves placed in both the supply and return lines to and from the heat pump. If the U-tube system was in operation, then the glycol mixture was pumped through the U-tube loop system collecting heat from the ground and exchanging that heat directly with the heat pump refrigerant. If the thermosiphon was in operation, then the flow from the U-tube ground loops was cut off by the ball valves, and the glycol mixture that had exchanged heat with the R-134a in the thermosiphon was pumped up to the attic instead. In this way, the flow of the glycol mixture to the heat pump was controlled.

Several sensors, including thermocouples, powermeters, and a flowmeter, were installed in unit 10. Temperature measurements were taken with T-type thermocouples. Continental Controls WNA-3Y-208-P WattNodes and 50 amp Current Transformers were implemented to measure power consumption. The glycol flow rate was measured

using a turbine-based flowmeter. A Campbell Scientific CR1000 data logger collected and stored the data from the sensors. A similarly instrumented four loop U-tube system was installed in an adjacent housing unit, unit 11. It served as a control for this study. The experimental setup was developed and installed under the direction of Christopher Workman as part of his Master of Science work, "Comparison of U-Tube Boreholes and a Thermosiphon on Heat Pump Performance in an Aquifer" [23].

Coefficient of Performance was used to assess the performance of the U-tube system. To find the COP of the system it was necessary to find the temperature difference between the glycol leaving the heat pump and the glycol entering the heat pump. It was also necessary to measure the power consumption of the system and the volume flow rate of the glycol mixture entering the heat pump. Thermocouples were placed on the inside of the pipe directly before and after the glycol exchanged thermal energy with the heat pump. A flowmeter recorded the volume flow rate of the glycol mixture, and powermeters measured the power consumption of the inline pump and the heat pump. These sensors were used to collect data over the course of two consecutive winters (2010-2011 and 2011-2012). The heating COP of the U-tube system was then calculated from the sensor readings.

For the subterranean heat transfer analysis, it was necessary to measure temperatures along the length of the thermosiphon pipe and along the length of one of the U-tube ground loops. Thermocouples were installed at depth increments of 25 feet along the outside surface of the thermosiphon pipe and along the outside surface of one of the U-tube ground loops. Days with cold mornings were selected, and on these days (November 22, 2010 and February 23, 2012) the thermosiphon and the U-tube system were run

continuously and independently until temperatures reached steady state. Then, each system was shut down. To find the heat transfer coefficient, temperature measurements were recorded once each system had been shut down. These temperature measurements were then analyzed and calculations were conducted as part of an *in situ* method for evaluating the convective heat transfer coefficient. This experimental setup along with the sensor locations is shown in Figure 3.1.

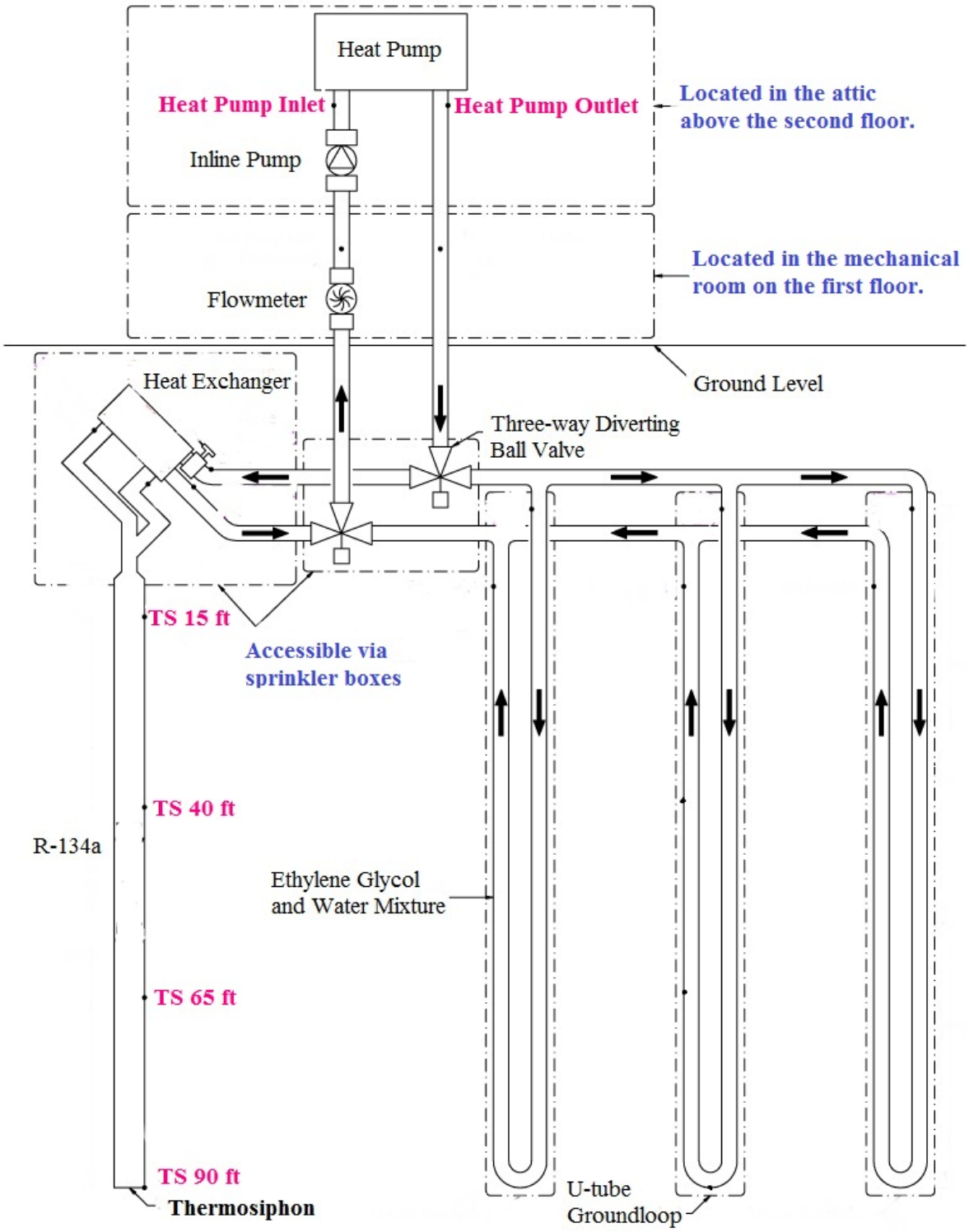

Figure 3.1: Experimental Setup. Thermocouple locations are labeled in pink. The installation of this experimental setup was part of Christopher Workman's thesis [23].

CHAPTER 4

RESULTS

4.1 Ground Source vs. Air Source

To assess U-tube performance, it first had to be determined that the ground was a more effective heat source than the air. For a heat pump operating at maximum theoretical efficiency or Carnot efficiency, COP can be defined by Equation 4.1.

$$COP_{HP,rev} = \frac{T_H}{T_H - T_L} \quad \text{(Equation 4.1)}$$

where:
T_H is the temperature of the space being heated in Kelvin (K) and
T_L is the temperature of the space from which heat is extracted (K).

As shown in Equation 4.1, the temperature of the heat source affects the heating performance of the system. Higher heat source temperatures result in greater heating performances. In order for ground source heat transfer to be more effective than air source heat transfer, ground temperatures must remain higher than ambient air temperatures. In this experiment, the ground source heat is transferred to a glycol mixture. The glycol mixture then exchanges its heat with a heat pump. Essentially, the glycol in the ground source system and the air in the air source system provide the same heat supply function. Both ambient air temperatures and glycol temperatures at the heat pump inlet were recorded. The results are plotted in Figure 4.1.

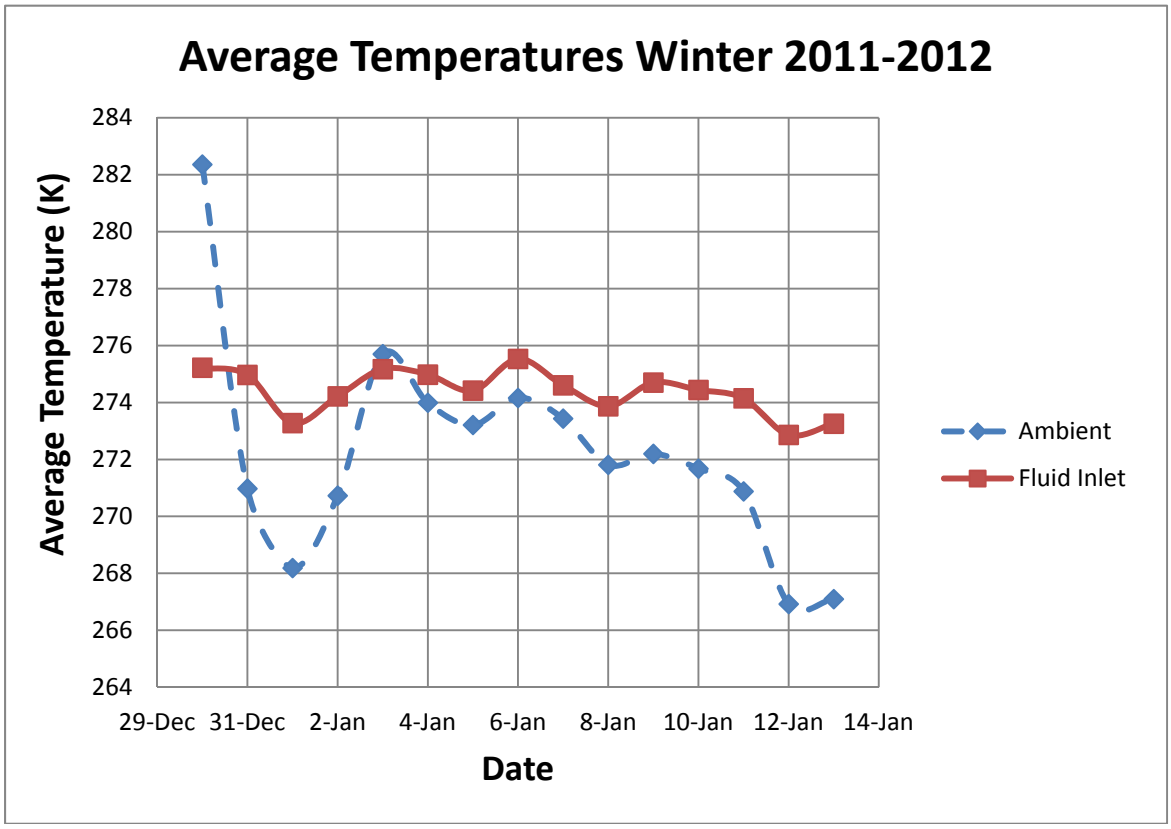

Figure 4.1: Daily Average Winter Temperatures. The solid line is the average daily temperature of the glycol at the heat pump inlet. The dashed line is the average daily ambient temperature at Snow Creek Cottages. The heat pump inlet is warmer than the ambient air, indicating that the ground is a more favorable heat source than the air.

In Figure 4.1 the heat pump inlet temperature remained higher than the ambient air temperature. This verifies that the ground was a more thermodynamically favorable heat source than the air during the time period of interest. The results are plotted on a smaller time scale in Figure 4.2. This plot also includes the heating load to show the relationship between heating load, ambient air temperature, and temperature of glycol entering the heat pump. As expected, the heating load decreased as the ambient temperature increased. The temperature measurements used for Figure 4.2 were taken directly after the U-tube system had been activated.

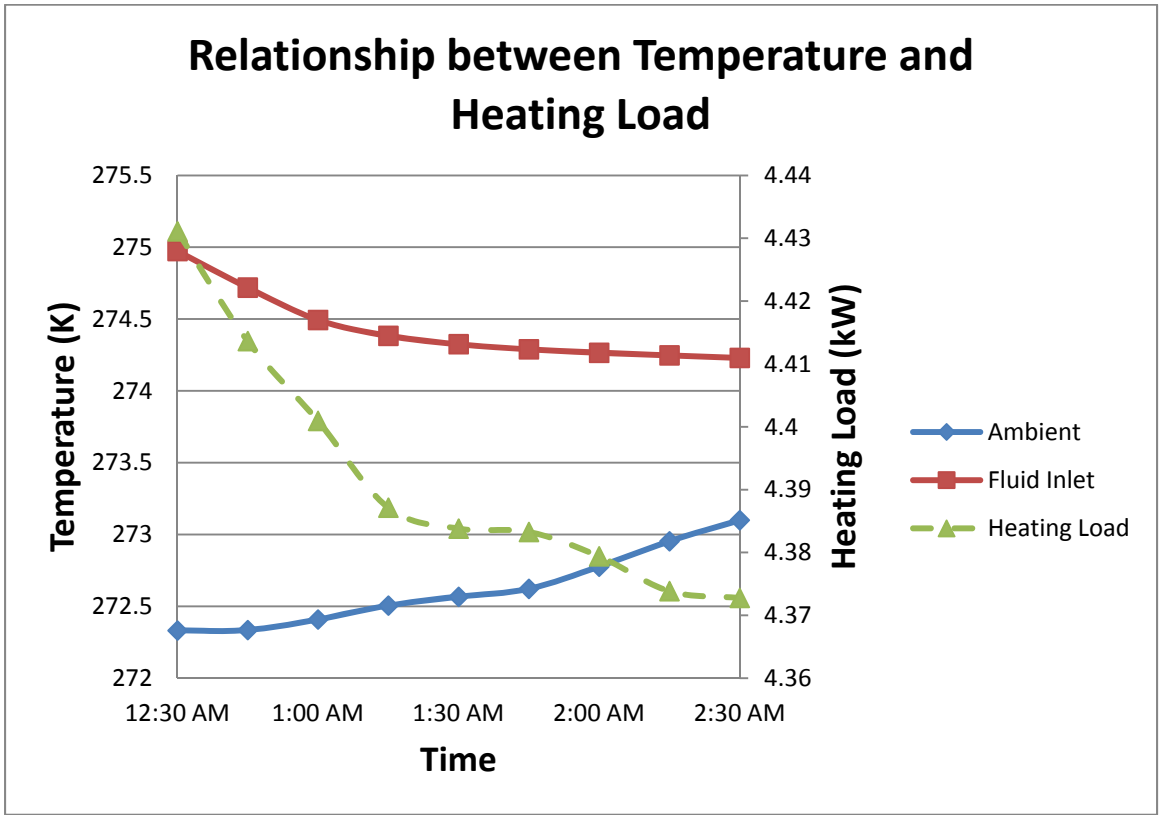

Figure 4.2: Relationship between Ambient Temperature, Heating Load, and Fluid Inlet Temperature. The temperature difference between ambient temperature and fluid inlet temperature decreases with time.

The findings of Figure 4.1 are reinforced in Figure 4.2; the ground is a more effective heat source than the air. Also, when the U-tube system was activated, the heat pump fluid inlet temperature decreased with the most significant drop occurring within the first 45 minutes. What was initially a 3 K difference between ambient temperature and fluid inlet temperature shrank to a 1 K difference 2 hours after the system had been turned on. This decrease in temperature difference indicates that as heat was continuously taken from the ground, the efficiency of the ground source system decreased somewhat, but as illustrated in Figure 4.1, the ground still remained a more thermodynamically favorable heat source than the air for the duration of the heating season.

4.2 Performance

The warmer ground temperatures indicated that a relatively high Coefficient of Performance was plausible, but this was not necessarily the case. Equation 4.1 only applies for a heat pump operating at maximum theoretical efficiency. The heat pump in this study is not operating at maximum theoretical efficiency. In this case, COP is essentially the ratio of the thermal energy output to the electrical energy input. For the U-tube system, the work input includes the work necessary to pump the glycol up to the heat pump and also the work necessary to operate the heat pump. The heat output was the heat transferred to the building. The COP can be described by the following equations:

$$COP_{HP} = \frac{Q_H}{W_{net}} \quad \text{(Equation 4.2)}$$

$$COP_{HP} = \frac{\dot{W_{net}} + \dot{Q_L}}{\dot{W_{net}}} \quad \text{(Equation 4.3)}$$

where:
Q_H is the heat transferred to the space being heated,
$\dot{W_{net}}$ is the rate of work input in kilowatts (kW), and
$\dot{Q}_L$ is the rate of heat transfer from the glycol to the heat pump (kW).

Based on the placement of sensors, Equation 4.3 was judged to be more practically applicable than Equation 4.2. The heat transfer rate from the glycol to the heat pump was calculated from the Equation 4.4:

$$\dot{Q}_L = c_p \rho \dot{V} \Delta T \quad \text{(Equation 4.4)}$$

where:
c_p is the specific heat of the glycol solution in kilojoules per kilogram degree Kelvin (kJ/kg-K),
ρ is the density of the glycol solution in kilograms per cubic meter (kg/m^3),

$\dot{V}$ is the volume flow rate of the glycol solution in cubic meters per second (m^3/s), and ΔT is the temperature difference between the glycol entering the heat pump and the glycol exiting the heat pump (K).

The operating COP for the U-tube system in unit 10 was calculated from Equation 4.3 and Equation 4.4 using sensor measurements. The COP was averaged daily over the course of three different time periods: from November 24, 2010 to December 22, 2010 (Figure 4.3), from February 14, 2011 to March 4, 2011 (Figure 4.4), and from December 30, 2011 to January 13, 2012 (Figure 4.5). For comparative purposes, the COP was also calculated and averaged daily for the U-tube system in unit 11 from February 15, 2011 to March 4, 2011 (Figure 4.6). These COP values were found while the U-tube system was running. The COP results are tabulated in Table 4.1.

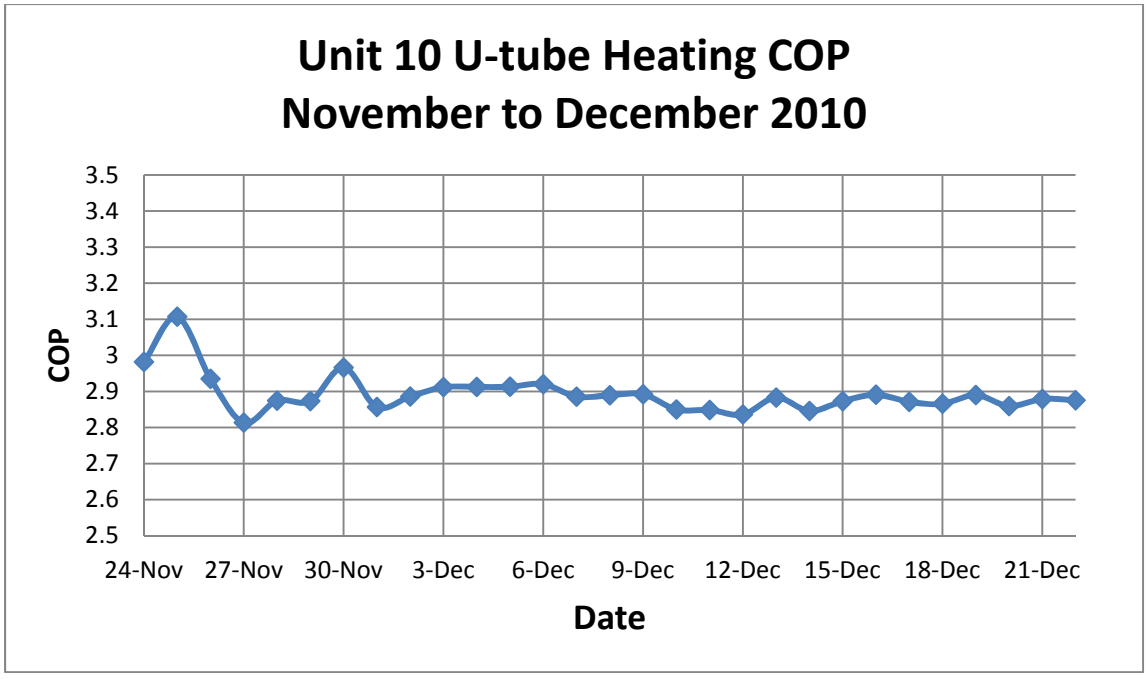

Figure 4.3: Unit 10 U-tube COP during Late 2010. This graph reflects data taken from November 24, 2010 to December 22, 2010.

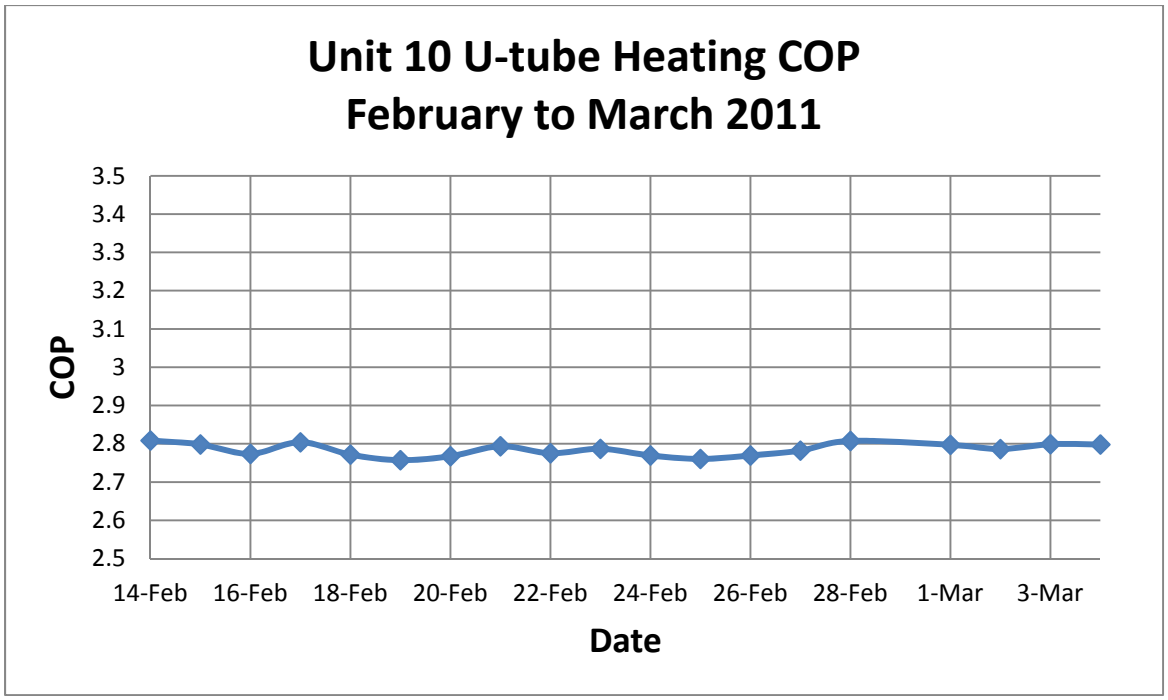

Figure 4.4: Unit 10 U-tube COP during Early 2011. This graph reflects data taken from February 14, 2011 to March 4, 2011.

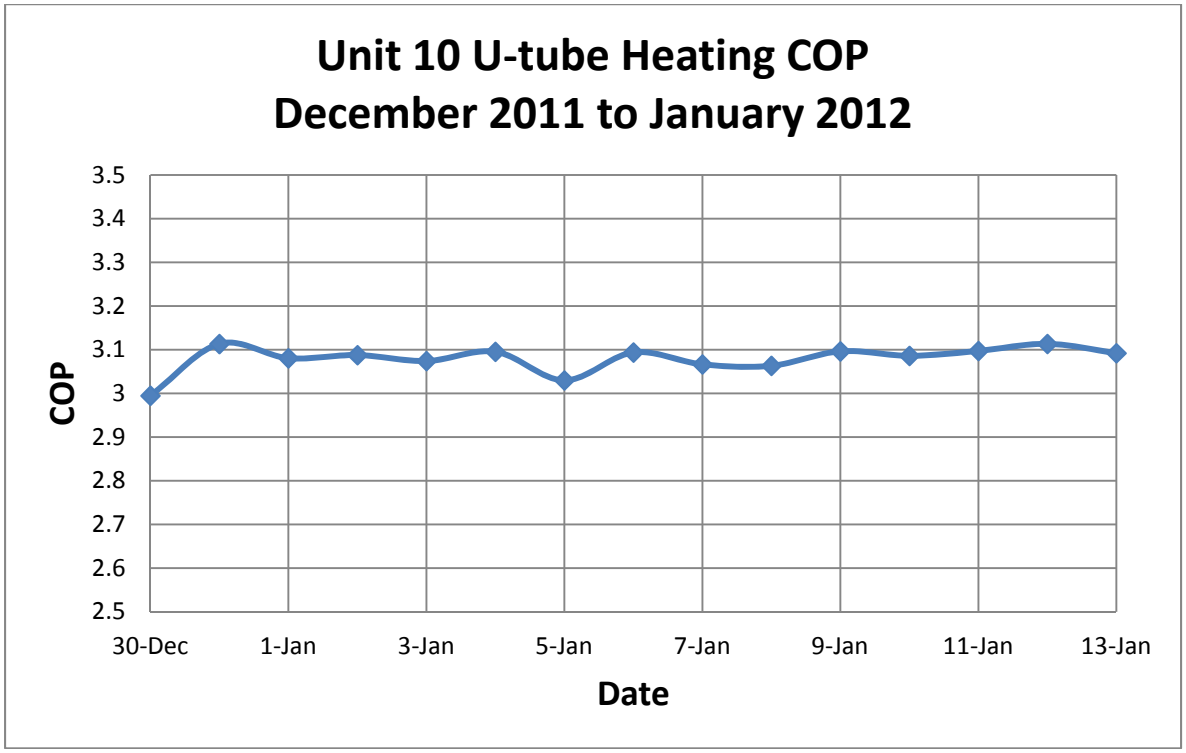

Figure 4.5: Unit 10 U-tube COP for Winter 2011-2012. This graph reflects data taken from December 30, 2011 to January 13, 2012. The COP for this heating season was higher than the COP for the previous heating season.

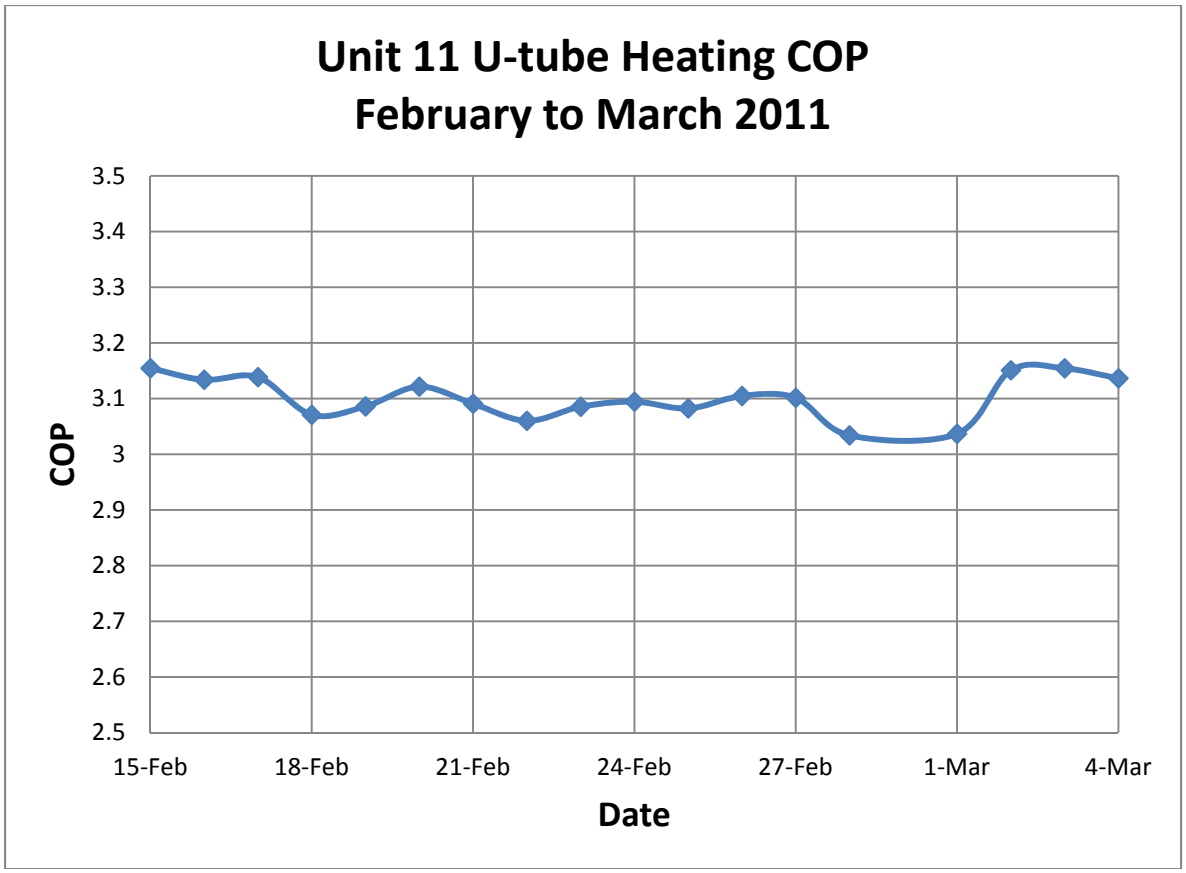

Figure 4.6: Unit 11 U-tube COP during early 2011. This graph reflects data taken from February 15, 2011 to March 4, 2011. The COP for unit 11 was higher than the COP for unit 10 during the same time period.

Table 4.1: COP Results.

COP Median Values

	Unit 10	**Unit 11**
November-December 2010	2.88	
February-March 2011	2.79	3.10
December 2011-January 2012	3.09	

Comparing Figure 4.4 and Figure 4.6 reveals that the unit 11 U-tube had a higher COP than the unit 10 system over the same time span. This COP difference is also highlighted in Table 4.1. From February to March 2011, the median COP for the unit 11 U-tube was 3.10. Over the same time span, the median COP for the unit 10 U-tube was 2.79. The higher COP in the unit 11 system can most likely be attributed to the fact that the unit 11 system has 4 ground loops, whereas, the unit 10 system has 3 ground loops. The greater thermal capacity of the unit 11 system probably resulted in a higher heating performance.

As demonstrated in Table 4.1, the COP was higher in the second heating season (the winter of 2011-2012) than in the first heating season (winter 2010-2011). In the first heating season, the COP mostly stayed between 2.75 and 2.90. From December 2011 to January 2012, the median COP was found to be 3.09. This could be the result of higher heat pump fluid inlet temperatures during the second heating season. The winter of 2011-2012 was significantly milder than the winter of 2010-2011. These warmer winter temperatures led to higher ground temperatures. Higher ground temperatures resulted in higher fluid inlet temperatures. The fluid inlet temperatures for each heating season are graphically depicted in Figure 4.7. Looking at Figure 4.7, the fluid inlet temperatures during the second heating season (median of 277 K) were consistently higher than the fluid inlet temperatures during the first heating season (median of 274 K). Based on this information, the higher U-tube heating performance during the second heating season was most likely the result of higher heat pump fluid inlet temperatures during the second heating season. This again illustrates the correlation between fluid inlet temperature and heat pump performance.

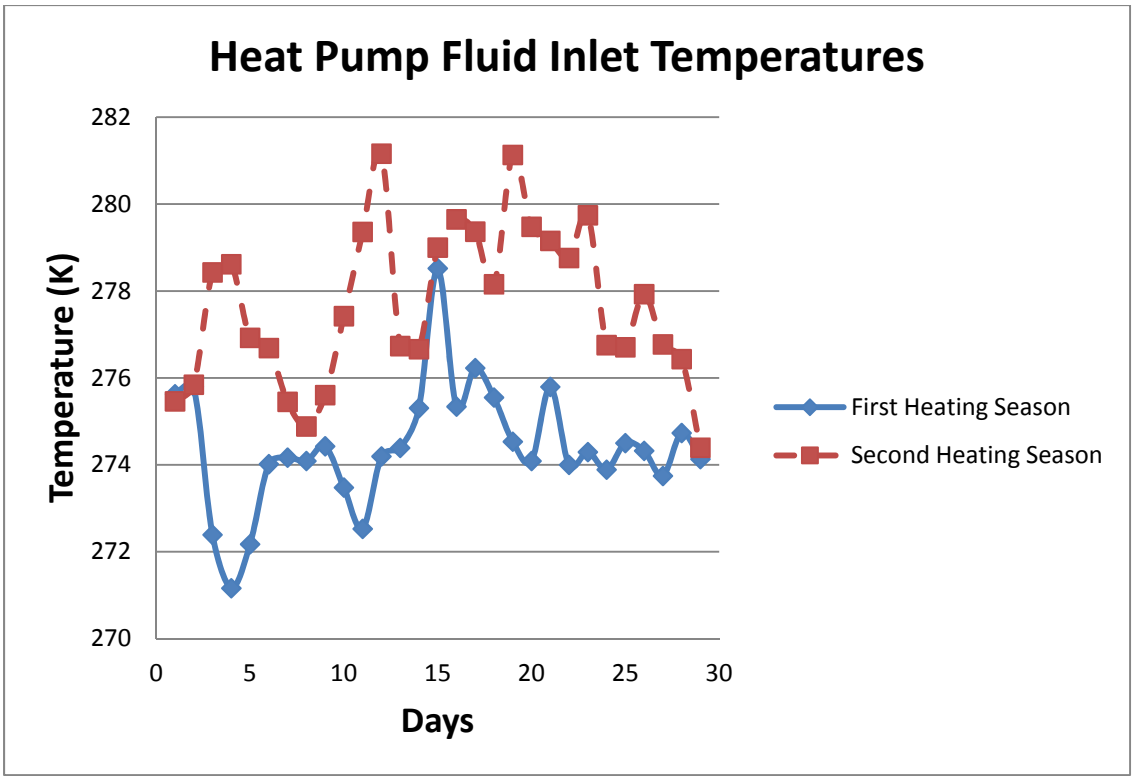

Figure 4.7: Heat Pump Fluid Inlet Temperatures. The heat pump fluid inlet temperatures for the second heating season were consistently higher than the temperatures during the first heating season.

Over the course of the two heating seasons, the operating COP of the U-tube remained between 2.75 and 3.1. This falls short of expectations found in the literature that have estimated the COP of GSHP systems to be between 3 and 5 [6, 12]. The higher COP values found in the literature could be due to the fact that some of these studies did not take into account the power consumption of the inline pump. Taking into account the power consumption of the inline pump decreases COP by about 0.4. Figure 4.8 shows the COP decrease resulting from the power consumption of the inline pump. Some of the performance advantage gained from warmer ground temperatures was lost as a result of the work input necessary to transport the glycol mixture to the attic.

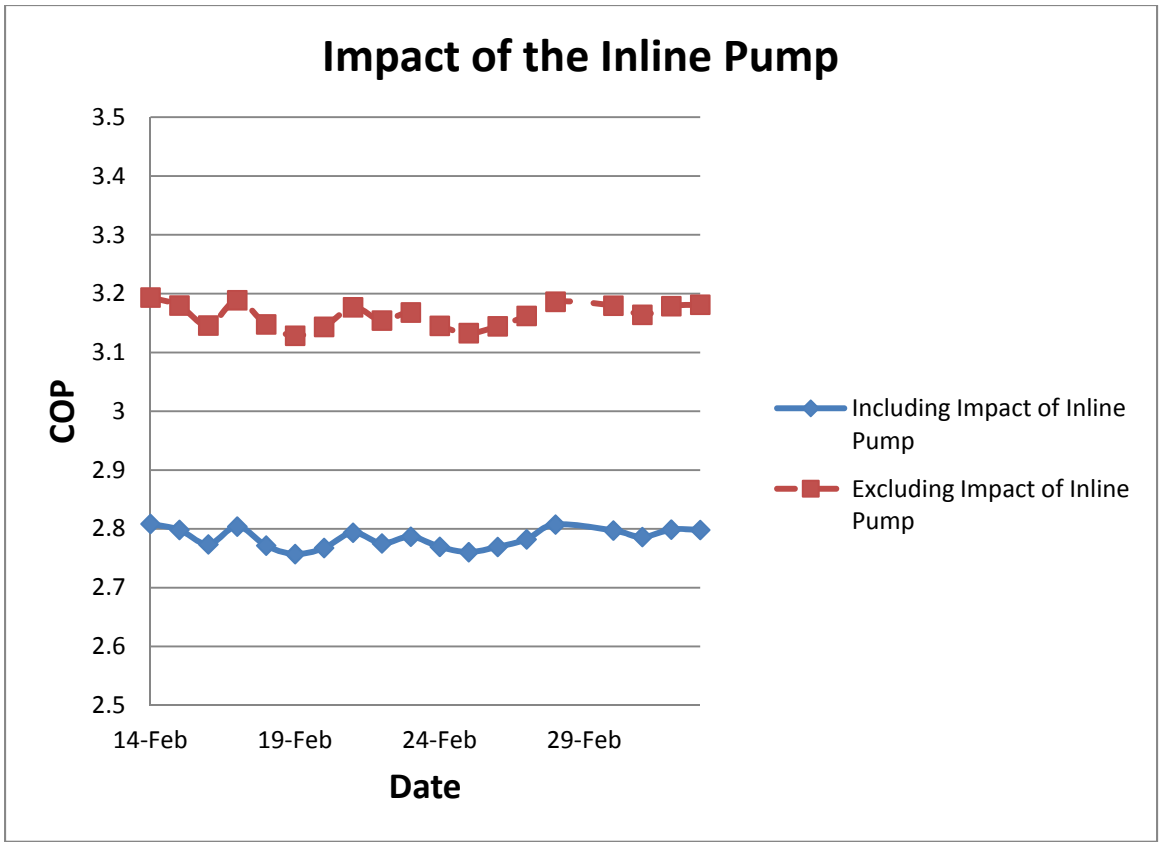

Figure 4.8: Impact of Inline Pump on Performance. This graph reflects data taken from February 14, 2011 to March 4, 2011. Including the power consumption of the inline pump in the COP calculations results in a COP drop of about 0.4.

Other inefficiencies may have adversely affected the U-tube performance as well. The piping is made from HDPE, a fairly inexpensive material that can be manufactured in long lengths, but it is also a relatively poor conductor. The thermal conductivity of HDPE is about ten times less than that of the soil. This results in poor heat transfer between the soil and the piping network. To overcome this issue, deeper boreholes are drilled, and the pipes are sealed with thermal grout. Another inefficiency is due to the proximity of the vertical legs of the U-tube ground loop. If the pipes are close enough, only a single borehole is necessary, saving money. The proximity does, however, allow for unwanted heat exchange between the vertical legs of the U-tube ground loop. During the heating

season, some of the heat coming out of the ground will be transferred from the return leg to the supply leg decreasing the temperature of the returning fluid and reducing the efficiency of the heating process. The same is true during the cooling season. Getting rid of or reducing these inefficiencies could improve the performance of the vertical U-tube GSHP.

In its present form, the U-tube system is relatively expensive to install. In the United States, heating and cooling loads are measured in tons. One ton of cooling load is equal to the amount of cooling provided by 1 ton of ice. One ton of heating or cooling load is equivalent to 3.51 kW. A typical residential building requires approximately 3 tons (10.5 kW) of heating and cooling load. Installation of a GSHP system to meet this requirement costs between $9,000 and $12,000. The installation of a high-efficiency natural gas furnace to meet this requirement costs between $7,000 and $10,000. Installation of an air source heat pump or a low-efficiency natural gas furnace with a comparable heating capacity costs about $4,000 [8]. Of these systems, the U-tube GSHP is the most expensive to install. As illustrated in Figure 4.1 and Figure 4.2, an ASHP would not be very effective in a cold climate such as Park City, Utah. In Utah, 85% of homes are heated using natural gas [1]. Also, coal is the predominant source of electricity generation in Utah. It is important to note that natural gas is about 3 times cheaper than coal-generated electricity and burns much cleaner than coal. Natural gas emits 50% less carbon dioxide than coal [1]. The heating COP of this particular U-tube system was found to be approximately 3. Compared with natural gas, the annual cost comes out to be about the same. As such, the U-tube GSHP, when used only for heating purposes, will not result in an emission reductions or a cost savings when compared to a high-efficiency

natural gas furnace. The high relative installation cost of this particular U-tube GSHP will not be recouped in energy cost savings when compared to a typical heating system.

For this study, COP was not used to evaluate the thermosiphon. The thermosiphon in a passive mode does not require an inline pump. However, in this experiment, an inline pump was employed to transport the glycol mixture from the heat exchanger to the attic. Also, the thermosiphon was only in operation for approximately 8 hours. The U-tube, on the other hand, was in operation for the duration of two complete heating seasons. As such, the COP of the thermosiphon in this case does not accurately reflect the performance of the thermosiphon. Instead, the COP assessment was confined to the U-tube system.

A different method was used to assess the performance of the thermosiphon. While the thermosiphon was running, temperature measurements were taken, and the heat transfer from the glycol solution to the heat pump was calculated from Equation 4.4. Given that the U-tube system is 3 times longer than the thermosiphon, the heat transfer results were normalized per unit length. These normalized results are presented in Figure 4.9.

From Figure 4.9, it appears that the heat transfer rate per unit length associated with the thermosiphon is approximately 2.33 times greater than the heat transfer associated with the U-tube. Overall, the thermosiphon more efficiently supplied heat from the piping network to the heat pump.

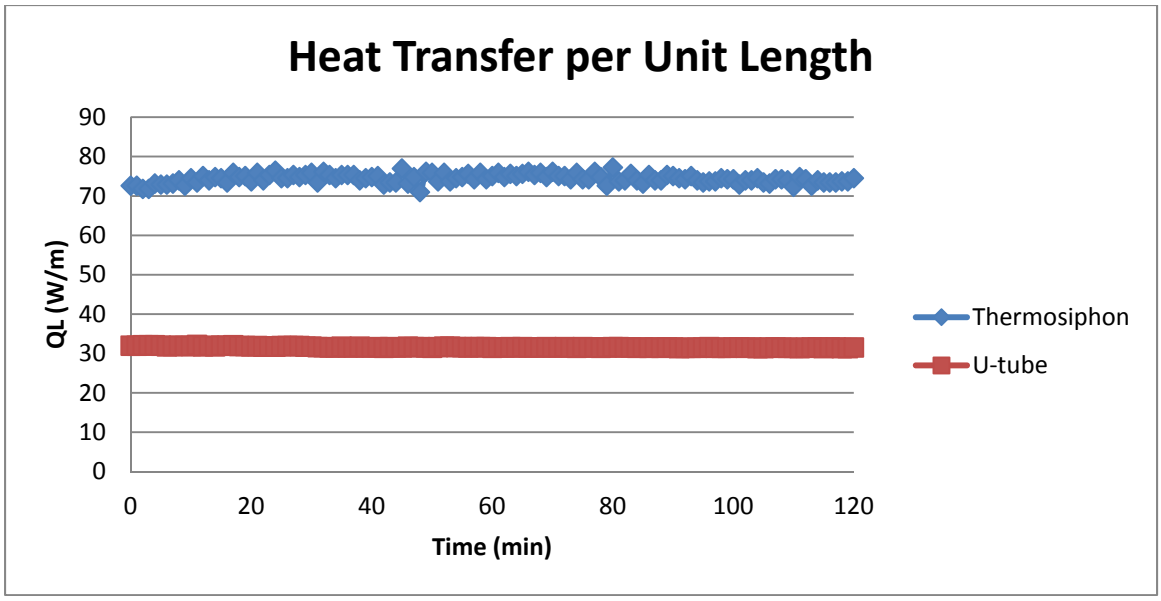

Figure 4.9: Heat Transfer per Unit Length. The heat transfer per unit length associated with the thermosiphon was about 2.33 times greater than the heat transfer associated with the U-tube.

4.3 Heat Transfer Analysis

On November 22, 2010, both the thermosiphon and the U-tube system were operated continuously for several hours. At about 10:00 am, the U-tube system was turned on. At about 2:30 pm the system was shut down and the thermosiphon was turned on. The thermosiphon was shut down at approximately 5:30 pm. The temperature response of each system was analyzed. These transients are shown in Figure 4.10 and Figure 4.11.

It was observed during the operation of each system that temperatures on the outside wall of the piping network became relatively constant with time. This indicated that the heat transfer to the thermosiphon and the U-tube was being matched by the heat transfer from adjacent soil regions. With those soils being permeable and the local hydraulic gradient being large, convective heating from flowing groundwater was most likely responsible for this observation.

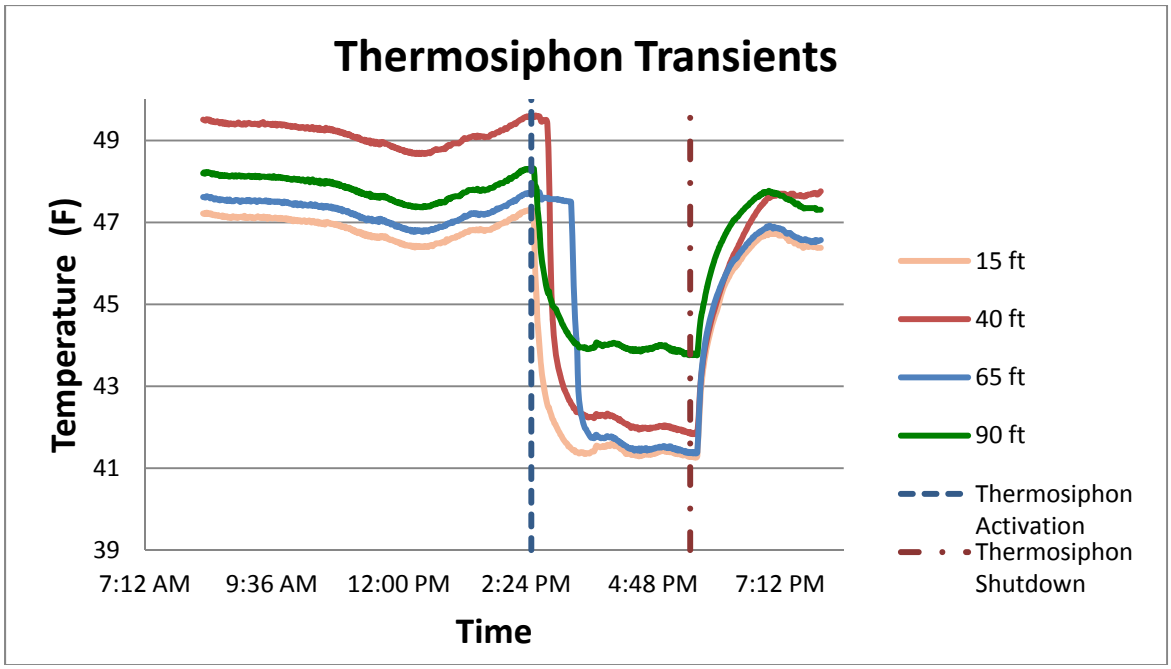

Figure 4.10: Thermosiphon Transients. Data from November 22, 2010. The temperature of the soil around the thermosiphon decreases when the thermosiphon is activated. When it is shut down, the temperature of the soil rebounds.

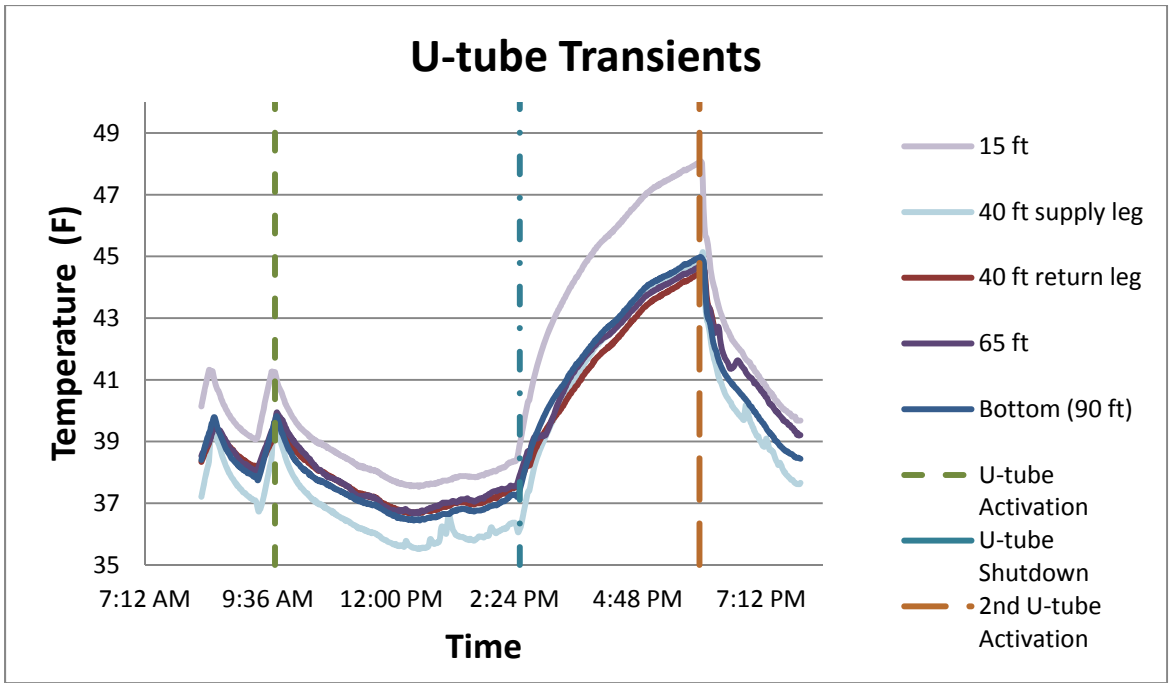

Figure 4.11: U-tube Transients. Data from November 22, 2010. The temperature of the soil around the U-tube decreases when the thermosiphon is activated. When it is shut down, the temperature of the soil rebounds.

A conceptual heat transfer model was developed based on the temperature responses shown in Figure 4.10 and Figure 4.11. In developing this model, the heat transfer coefficient was assumed to be constant around the entire pipe. Based on this assumption and looking only at convective heat transfer from flowing groundwater, a subterranean heat exchanger (a thermosiphon pipe or a U-tube ground loop) in the center of a borehole sealed with thermal grout that is convectively heated by the flow of groundwater is the conceptual model that was developed (Figure 4.12).

This model was used as the basis in developing a method for inferring the heat transfer coefficient from only temperature data. The mathematical development of this method starts with the heat equation. Assuming that the grout has a very low permeability compared to the surrounding soil and assuming that the groundwater flow is axisymmetric and one-dimensional, the heat equation governs the flow of thermal energy in the grout:

$$\frac{1}{r}\frac{\partial(r\frac{\partial T}{\partial r})}{\partial r} = \frac{1}{\alpha_g}\frac{\partial T}{\partial t} \qquad \text{(Equation 4.5)}$$

where:
r is radial position,

T is temperature,

t is time, and

α_g is the thermal diffusivity of the thermal grout (this form of the heat equation assumes constant grout and soil properties).

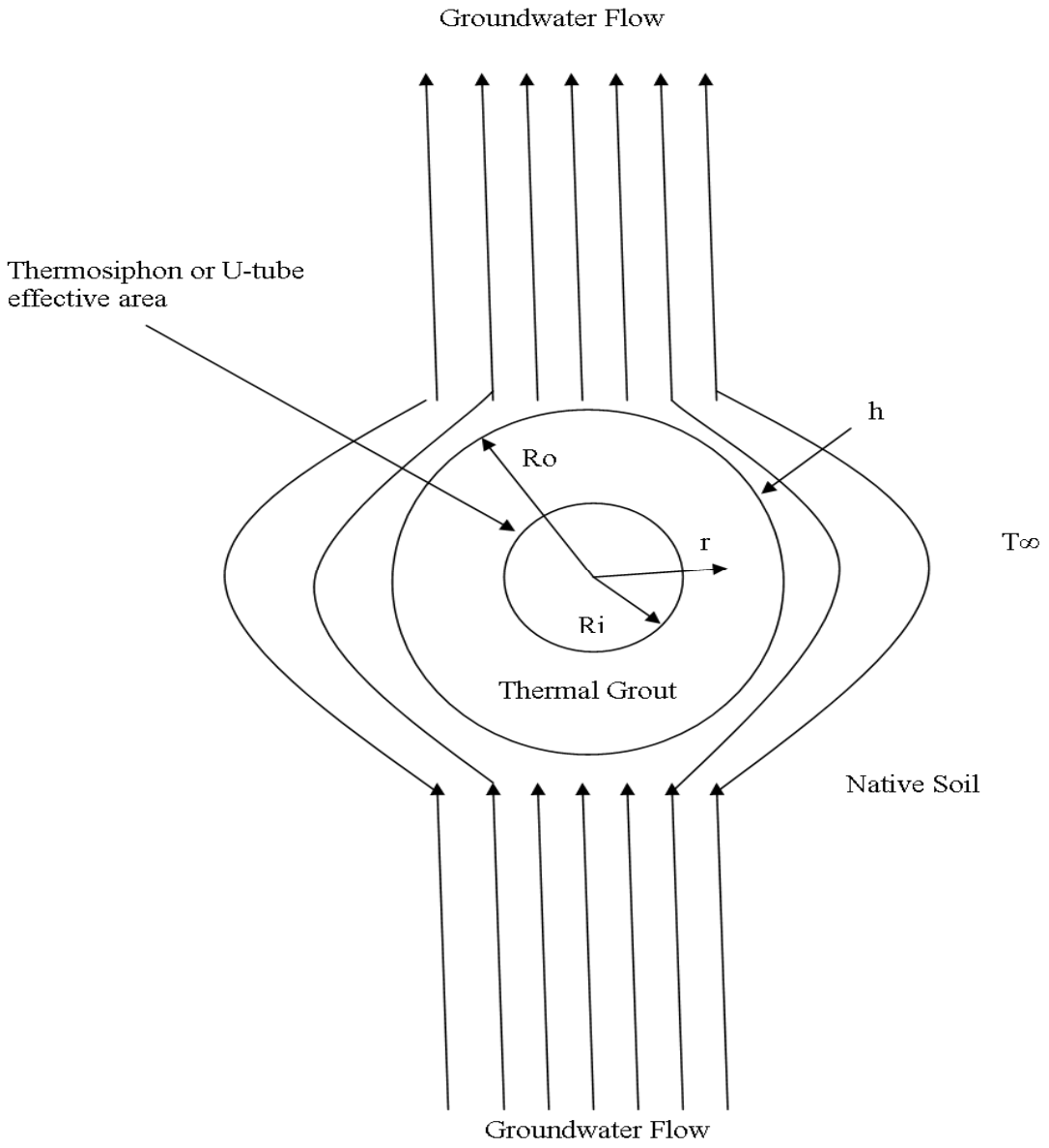

Figure 4.12: Conceptual Heat Transfer Model.

Two theoretical descriptions of the heat transfer from the soil to the thermosiphon are of value in this development: the convective heat transfer rate from the flowing groundwater to the outer surface of the grout and the transient response of the grout to changes in the thermosiphon operation. Transient thermosiphon data can be used to analyze both these descriptions once the thermosiphon has been cut-off from the flow of

the ethylene glycol solution (cooling of the R-134a at the top of the thermosiphon will cease).

Consider the heat transfer from a thermosiphon under steady-state conditions. The heat transfer from the inside surface of the grout (outside surface of the thermosiphon pipe) per unit length of pipe, *q'*, is defined by Fourier's law:

$$q' = -2\pi k_g \left(r \frac{\partial T}{\partial r} \right)\Bigg|_{r=R_i} \qquad \text{(Equation 4.6)}$$

where:
k_g is the thermal conductivity of the grout and
R_i is the inside radius of the grout (outside radius of the thermosiphon).

The heat transfer from the flowing groundwater to the outside of the grout is specified by Newton's law of cooling:

$$q' = 2\pi R_o h(T\big|_{r=R_o} - T_\infty) = -2\pi k_g \left(r \frac{\partial T}{\partial r} \right)\Bigg|_{r=R_o} \qquad \text{(Equation 4.7)}$$

where:
R_o is the outside radius of the grout,
h is the heat transfer coefficient, and
T_∞ is the ambient temperature of the groundwater.

Under steady-state conditions, Equation 4.5 reduces to an ordinary differential equation (ODE) since *T* is only a function of *r*. The variation of temperature with respect to radius*, T(r)*, is obtained from the ODE using separation of variables, and integrating twice with respect to *r*. The two resulting constants of integration are defined by the boundary conditions (BCs) of the inside and outside surfaces of the grout. The boundary condition at the inside surface of the grout is the heat flux described by Equation 4.6. The

boundary condition at the outside surface of the grout is the equality of the conductive heat flux to the outside radius of the grout and the convective heat flux from the flowing groundwater (Equation 4.7). The steady-state temperature distribution can be written as:

$$T(r) - T_\infty = \frac{q'}{2\pi k_g}\left[\ln\left(\frac{R_o}{r}\right) + \frac{1}{Bi}\right] \qquad \text{(Equation 4.8)}$$

where the Biot number (Bi) is defined as:

$$Bi = \frac{hR_o}{k_g} \qquad \text{(Equation 4.9)}$$

The transient solution of interest in this study is the response of the grout once heat transfer to the thermosiphon is reduced to zero. The transient solution can be found by solving Equation 4.5 using the fact that no heat is being transferred to the thermosiphon as the first BC:

$$-2\pi k_g\left(r\frac{\partial T}{\partial r}\right)\Bigg|_{r=R_i} = 0$$

Newton's Law of Cooling as the second BC:

$$Bi(T|_{r=R_o} - T_\infty) = -\left(r\frac{\partial T}{\partial r}\right)\Bigg|_{r=R_o}$$

and the steady state temperature distribution as the initial condition:

$$F(r) = T(r) - T_\infty = \frac{q'}{2\pi k_g}\left[\ln\left(\frac{R_o}{r}\right) + \frac{1}{Bi}\right]$$

From these boundary and initial conditions, the solution was found to be:

$$T(r,t) - T_\infty = \sum_{m=1}^{\infty} C_m R(\lambda_m, r) \exp(-\lambda_m^2 Fo) \qquad \text{(Equation 4.10)}$$

where:

$$R(\lambda_m, r) = J_o(\lambda_m\, r/R_o) Y_1(\lambda_m \beta) - Y_o(\lambda_m\, r/R_o) J_1(\lambda_m \beta)$$

The ratio of the inside to outside grout radii (β) is:

$$\beta = \frac{R_i}{R_o}.$$

The Fourier number (Fo) is defined as:

$$Fo = \frac{\alpha_g t}{R_o^2},$$

where:
α_g is the thermal diffusivity of the grout and
t is the characteristic time.

The eigenvalues, λ_m, are found from the roots of the following characteristic equation:

$$J_1(\lambda_m) Y_1(\lambda_m \beta) - Y_1(\lambda_m) J_1(\lambda_m \beta) - \frac{Bi}{\lambda_m}\left[J_o(\lambda_m) Y_1(\lambda_m \beta) - Y_o(\lambda_m) J_1(\lambda_m \beta)\right] = 0$$

(Equation 4.11)

The constants, C_m, are defined by:

$$C_m = \frac{\int_{R_i}^{R_o} rR(\lambda_m, r) F(r) dr}{\int_{R_i}^{R_o} rR^2(\lambda_m, r) dr}$$

For the purpose of this study, the steady state temperature distribution, Equation 4.8, and the value of the first eigenvalue, λ_1, are the most important theoretical results. The first eigenvalue defines the rate of temperature change once the Fourier number exceeds

0.2 since subsequent m = 2, 3, ⋯ ∞ eigenvalues are much larger resulting in much faster decay times for subsequent terms of the summation, as shown in Equation 4.10. From the form of the characteristic equation, Equation 4.11, it is expected that there will be unique relationships among λ_1, β, and *Bi.* The possible eigenvalues were found using excel. The three values of β were three possible ratios of the inside to outside grout radius. The exact grout ratio was not known, but these values served as estimates. By analyzing the transient data obtained once the thermosiphon condenser was no longer cooled, the observed temperature decay rate can be matched to the theoretical value to determine the effective *Bi*, and thus the effective convective heating rates at different locations. Table 4.2 lists the first eigenvalue for various values of the Biot number and three different ratios of the inner to the outer grout radii. This relationship is rendered in graphical form in Figure 4.13.

Table 4.2: Values of λ_1 for various Biot numbers. $\beta = R_i/R_o$.

Relationship Between λ_1, β, and Bi

Bi	λ_1		
	$\beta = 0.2$	$\beta = 0.42$	$\beta = 2/3$
0.01	0.14	0.16	0.19
0.02	0.2	0.22	0.27
0.05	0.32	0.35	0.42
0.1	0.45	0.49	0.6
0.2	0.63	0.685	0.84
0.5	0.96	1.055	1.31
0.7	1.12	1.227	1.53
1	1.29	1.43	1.8
1.3	1.43	1.59	2.02
2	1.66	1.87	2.42
3.5	1.94	2.23	2.99
5	2.09	2.44	3.36
7.5	2.21	2.61	3.75
10	2.31	2.76	4
10,000	2.57	3.2	5.1

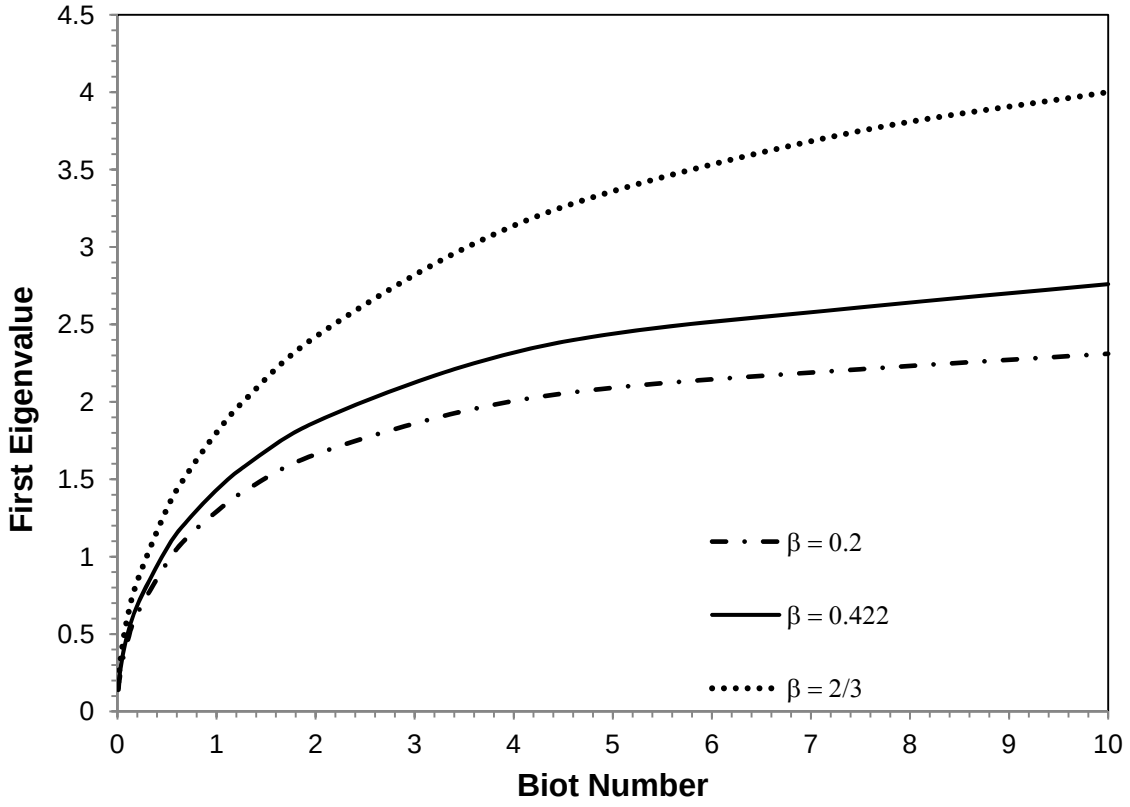

Figure 4.13: First Eigenvalue as a Function of the Biot Number. Different curves reflect different ratios of the inner to outer grout radii.

Temperature measurements during the heat up of the region around the thermosiphon and around the U-tube ground loop were analyzed to evaluate the observed temperature decay times and estimate the Biot number to determine the effective convective heat transfer coefficient between the grout and the flowing groundwater. These transient temperature profiles are shown in Figure 4.10 and Figure 4.11. As illustrated, the temperatures around both the U-tube system and the thermosiphon decreased rapidly when the system was activated. As soon as each system was shut down, the soil temperatures around that system rebounded to their original far field temperatures. As seen in Figure 4.11, the thermosiphon temperatures rebounded more quickly than the U-tube temperatures. The temperatures did not quite reach the far field temperatures within

the time span of interest. Eventually, these temperatures reached the far field temperatures, but the fact that they did not reach this temperature within the time span of interest indicates that heat was being removed from the surrounding soil regions while the thermosiphon and the U-tube were in operation.

Assuming the functional form of the temperature change with time is well-represented by the first term (m=1) of Equation 4.10 once the Fourier number is greater than 0.2, the observed temperature should change in a way that can be represented by the following exponential function:

$$\frac{T(R_o,t)-T_\infty}{T_i-T_\infty} = C_1 \exp(-\lambda_1^2 \frac{\alpha_g t}{R_o^2}) \qquad \text{(Equation 4.12)}$$

This temperature change occurred during the shutdown period of the thermosiphon. Taking the natural logarithm of both sides of Equation 4.13 yields a linear relationship between the natural logarithm of scaled temperature and time:

$$\ln\left(\frac{T(t)-T_f}{T(0)-T_f}\right) = -nt \qquad \text{(Equation 4.13)}$$

where:
t is the time after the thermosiphon shutdown,
T_f is the final steady state temperature, and
$T(0)$ is the initial temperature at $t=0$.

A plot of the natural logarithm of the scaled temperature versus time would produce data that would fall on a straight line with a negative slope n where:

$$n = \lambda_1^2 \frac{\alpha_g}{R_o^2} \qquad \text{(Equation 4.14)}$$

Such a plot was generated using data taken from Snow Creek Cottages. On November 22, 2010, at 2:30 pm, the thermosiphon was activated until 5:30 pm. The thermosiphon was then shut off. Temperature measurements were recorded and the normalized temperatures were fitted to a straight line. This curve-fit is shown in Figure 4.14. In fitting a straight line to the temperature data for each location, some extraneous data points were omitted. Early time data points were not considered since the Fourier numbers were small. Longer term data points were ignored since the uncertainty in the exact value of the far field temperature (T_∞) amplified the uncertainty of the ratio as T approached T_∞. T_∞ was assumed to be the temperature of the thermosiphon immediately before operation began. As time progressed, the exact value of T_∞ could have changed as ambient temperatures changed.

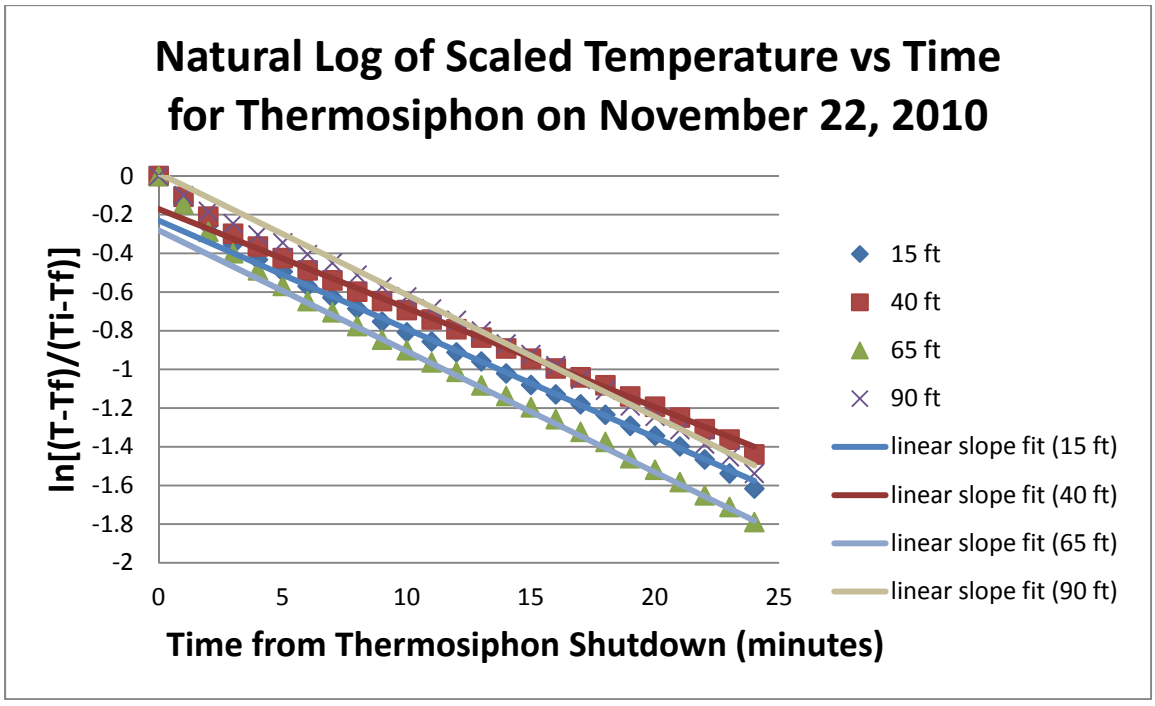

Figure 4.14: Natural Logarithm of Scaled Temperature vs Time for the Unit 10 Thermosiphon on November 22, 2010. The data shows heat-up of the soil once thermosiphon operation had stopped.

Once the slope of each curve-fit had been determined, Equation 4.14 was implemented to solve for the first eigenvalue. For the four locations where the outside surface of the thermosiphon pipes were instrumented with thermocouples (depths of 15 ft, 40 ft, 65 ft, and 90 ft), the best fit values of λ_1 ranged from 2.15 to 2.38. The ratio of the pipe outside diameter to the wellbore outside diameter (assumed to be the bit diameter) was calculated to be 0.42. Referring back to Figure 4.13, the effective Biot number for the convective heat transfer from the outside of the grout to the flowing groundwater was thus between 3 and 4.5. For this analysis, the Nusselt number (Nu) is the Biot number multiplied by the ratio of the thermal conductivity of the thermal grout (1.85 W/m^2) to the thermal conductivity of the local permeable soil (1.5 W/m^2) and then multiplied by a factor of two since the Biot number is based on the outside borehole radius, and the Nusselt number is based on the outside borehole diameter. From the experimental data, the Nusselt numbers around the thermosiphon were found to be between 7.2 and 10.8. The heat transfer coefficient, h, was then calculated from Equation 4.15:

$$h = \frac{Nu_D k_s}{D} \qquad \text{(Equation 4.15)}$$

where:
Nu_D is the Nusselt number on a diameter basis,
D is the outside grout diameter (m), and
k_s is the thermal conductivity of the local permeable soil (W/m-K).

From Equation 4.15, the heat transfer coefficient of the thermosiphon was calculated to be between 96 and 144 W/m^2-K.

A different result was obtained for the U-tube boreholes. These temperature measurements were recorded on the same day, November 22, 2010. About 10:00 am, the U-tube system was turned on. It was shut down at 2:30 pm. The transient response was then analyzed in the same way as for the thermosiphon. The natural logarithm of scaled temperature as a function of time for the U-tube system after shutdown is shown in Figure 4.15. The accuracy of this slope fit was confirmed with data recorded on February 23, 2012 (Figures 4.16 and 4.17).

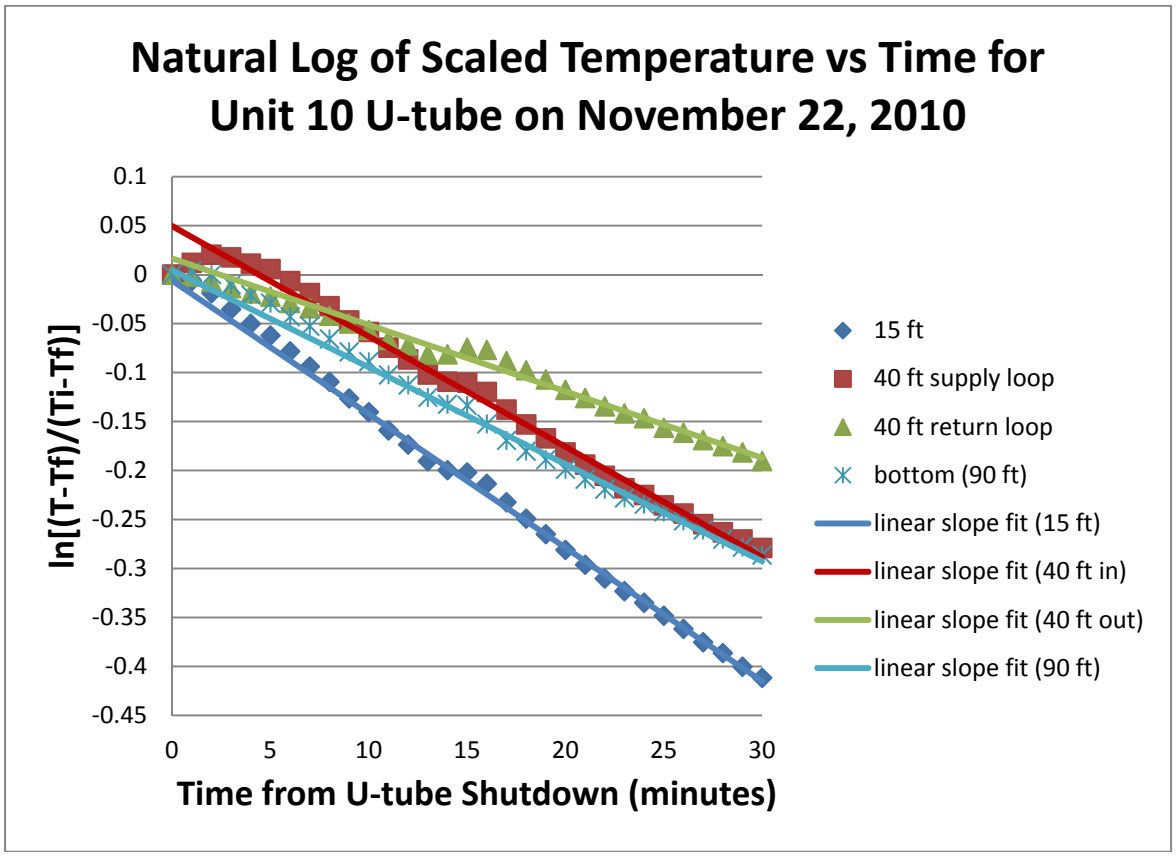

Figure 4.15: Natural Logarithm of Scaled Temperature vs Time for Unit 10 U-tube on November 22, 2010. The data shows heat-up of the soil once U-tube operation had stopped.

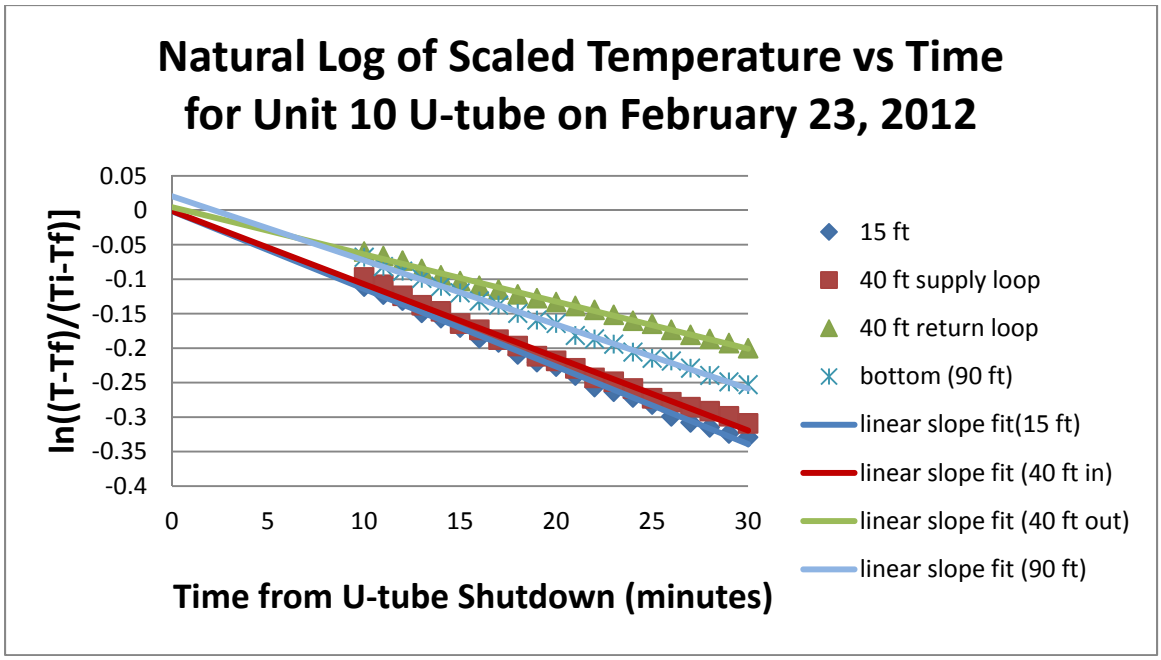

Figure 4.16: Natural Logarithm of Scaled Temperature vs Time for Unit 10 U-tube on February 23, 2012. The data shows heat-up of the soil once U-tube operation had stopped. This data matches well with the earlier results found on November 22, 2010.

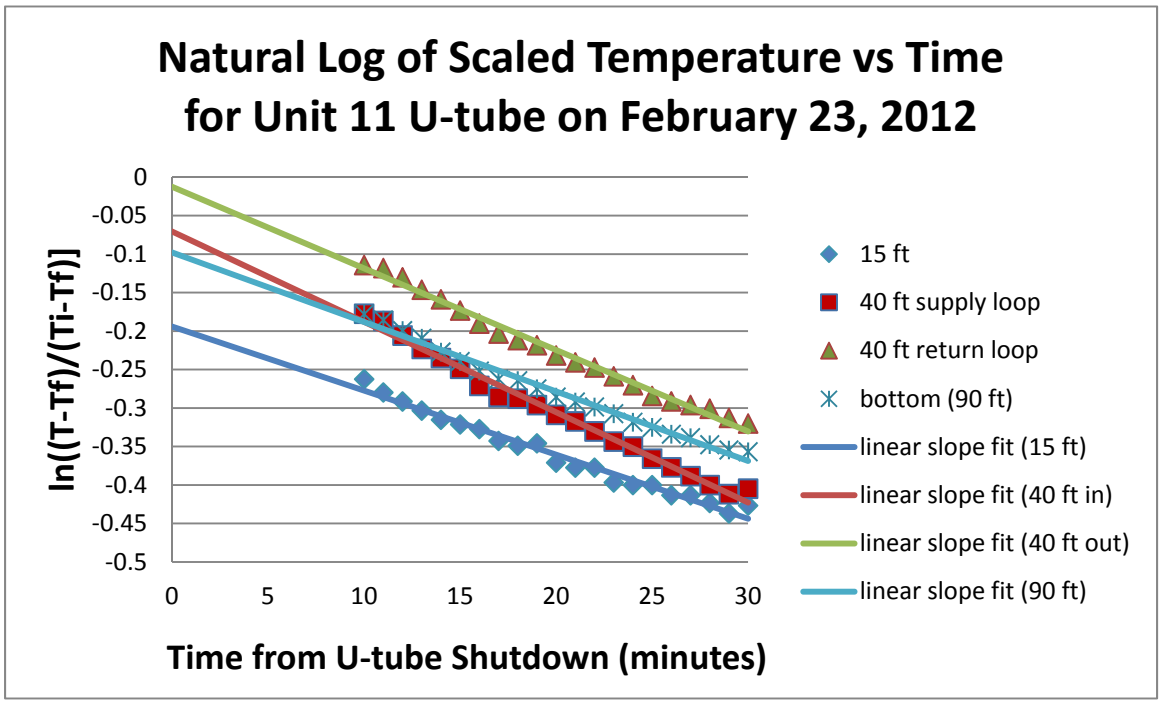

Figure 4.17: Natural Logarithm of Scaled Temperature vs Time for Unit 11 U-tube on February 23, 2012. The data shows heat-up of the soil once U-tube operation had stopped. This plot confirms the results found for the Unit 10 U-tube.

From the linear curve fits for the U-tube, best fit values of λ_1 ranged from 0.785 to 1.028. From these eigenvalues and referring back to Figure 4.13, Biot numbers near the U-tube boreholes were found to be between 0.25 and 0.45. In the same way as for the thermosiphon, the Nusselt numbers around the U-tube were determined to be between 0.62 and 1.1. Using Equation 4.16, the heat transfer coefficient between the U-tube grout and the flowing groundwater was found to be between 8 and 14.4 W/m^2-K. This range is on the same order of magnitude as air flowing across a cylinder.

Similar transients were observed in an instrumented unit 11 U-tube borehole about 8 meters away (Figure 4.17). The behavior of the unit 11 U-tube system confirmed the results found for the unit 10 U-tube system.

The outside convective heat transfer coefficient can also be estimated from convective heat transfer correlations for cylinders in cross-flow of low Prandtl number fluids. Since the ratio of the thermal boundary layer thickness to the momentum boundary layer thickness is large for low Prandtl number fluids, the far-field velocity field controls the convective transport more than cylinder wall boundary layer effects. Also, the far-field flow field for low Reynolds number flow around a cylinder is the same as the flow field near a cylinder in homogeneous porous media. Thus, low Reynolds number, low Prandtl number heat transfer correlations can be used to estimate the convective heat transfer coefficient between flowing groundwater and ground source heat exchangers.

In order to use these correlations, the groundwater velocity was estimated using Darcy's law:

$$V = K\left(\frac{dh}{dl}\right) \qquad \text{(Equation 4.16)}$$

where:

$\frac{dh}{dl}$ is the hydraulic gradient (the change in height [h] over the change in length [l]) and K is the hydraulic conductivity (m/s) given by:

$$K = \frac{k\rho g}{\mu}$$

where:
k is the permeability of the soil (m^2),
ρ is the density of the groundwater (kg/m^3),
g is the acceleration due to gravity (m/s^2), and
μ is the dynamic viscosity of the groundwater ($N\text{-}s/m^2$).

Based on the local stream gradient, the hydraulic gradient was estimated to be 2.2 E-03. The permeability of the soil was estimated to be 50 μm^2 since the soil logs at Snow Creek Cottages indicated the presence of gravel. From these parameters Darcy's law predicts a groundwater velocity of 7.6 E-07 m/s.

In cases of groundwater flow over a cylinder, the following Nusselt number correlation applies on a diameter basis [24]:

$$Nu_D = \frac{1}{.8237 - \ln(Re_D Pr)^{.5}} \quad \text{(Equation 4.17)}$$

where:
Re_D is the Reynolds number on a diameter basis and
Pr is the Prandtl number.

The Prandtl number multiplied by the Reynolds number is defined as the Peclet number (Pe_D). Equation 4.17 can thus be rewritten in the following form:

$$Nu_D = \frac{1}{.8237 - \ln(Pe_D)^{.5}} \quad \text{(Equation 4.18)}$$

The Peclet number can be defined as:

$$Pe_D = \frac{VD}{\alpha_s} \quad \text{(Equation 4.19)}$$

where:
V is the velocity of the groundwater (m/s),
D is the outside diameter of the thermal grout (m), and
α_s is the thermal diffusivity of the native soil (m^2/s) given by:

$$\propto_s = \frac{k_s}{\rho c_p}$$

where:
k_s is the thermal conductivity of the native soil (W/m-K),
ρ is the density of the groundwater (kg/m^3), and
c_p is the specific heat of the groundwater (kJ/kg-K).

This correlation applies for Peclet numbers less than 0.2. From Equation 4.19, the Peclet number was calculated to be at the upper limit of this range. For groundwater velocities much higher than those found on site, a different correlation would have to be used. From Equation 4.18, the theoretically Nusselt number for the U-tube system was calculated to be 0.65. On a diameter basis, the *in situ* method developed here inferred a U-tube Nusselt number between 0.62 and 1.1. The theoretical prediction fell within this range.

This was not the case for the thermosiphon. The experimental data inferred a thermosiphon Nusselt number that was 10 times greater than the theoretical prediction. Other empirical evidence may explain this discrepancy. On September 28, 2011, a string of thermocouples attached to cross-linked polyethylene tubing (PEX) was lowered into the thermosiphon pipe. Temperature measurements were taken and a subterranean temperature profile was found and plotted for the thermosiphon. These results are shown in Figure 4.18. It was assumed that the temperatures within the thermosiphon pipe would accurately reflect ground temperatures as the thermosiphon had not been operated in several months and was left off while the temperature measurements were being taken.

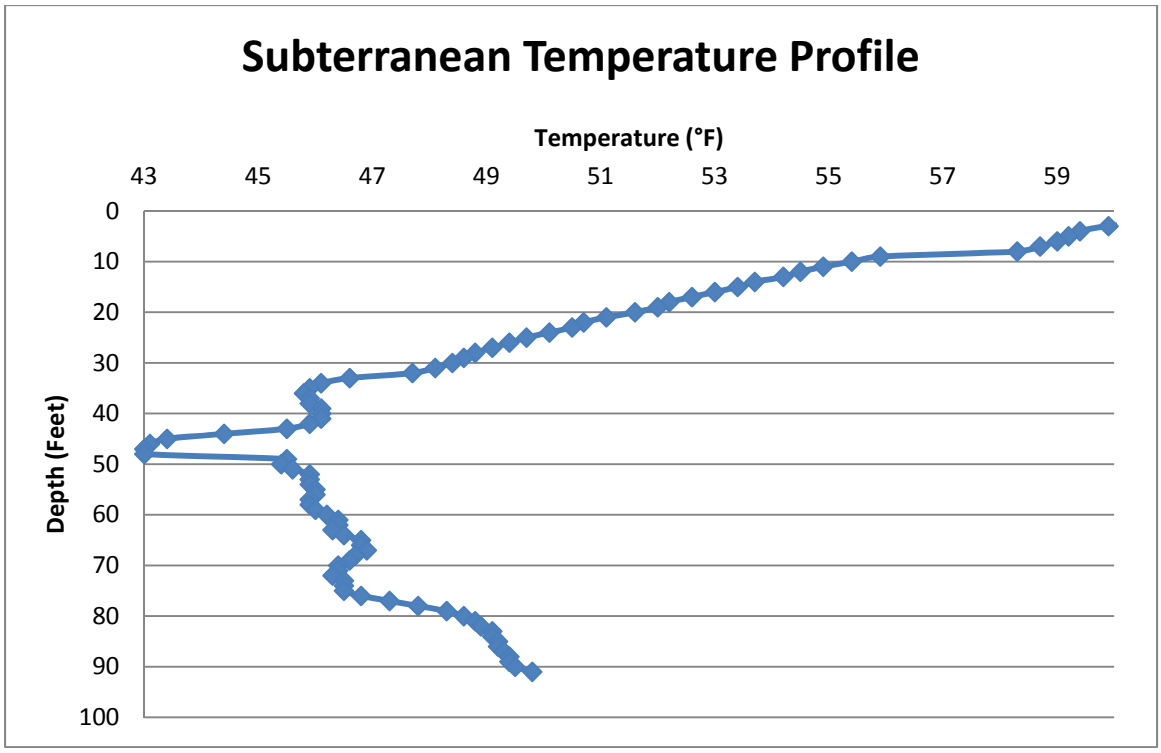

Figure 4.18: Subterranean Temperature Profile. These temperature measurements were recorded on September 28, 2011. The temperature varied significantly with depth.

As demonstrated in Figure 4.18, the underground temperature varied significantly with depth. In addition, different profiles were found for different times of year. The subterranean temperature profile was not constant. This suggests that the higher heat coefficients found for the thermosiphon were probably not a result of convective heat transfer from the outside of the pipe. Rather, they were an indication of the rapid heat transfer that occurred on the inside of the thermosiphon. Here is one plausible explanation. The fluid collecting at the bottom of the thermosiphon evaporated, absorbing heat from the ground. The less dense fluid rose. At around 50 feet, the temperature in the thermosiphon was found to be lower than the surrounding regions. At this point, the refrigerant condensed and transferred heat to this region of low temperature. At points of higher ground temperature, the fluid evaporated and rose. At points of lower ground

temperature, the fluid condensed and dripped down the walls of the pipe. In this way, the thermosiphon was redistributing heat in an attempt to achieve temperature uniformity along the length of the pipe.

By its nature, even when it was not exchanging heat with the heat pump, the thermosiphon still exchanged heat with the surrounding ground. If there was a soil region that was at a higher temperature than other regions, the thermosiphon transferred heat from that region to the cooler regions along the length of the thermosiphon. In this study, the rebound of soil temperatures back to far field temperatures was analyzed. It was observed that the soil regions in the vicinity of the thermosiphon rebounded much more quickly than the soil in the vicinity of the U-tube. The data gave the appearance that an extremely high rate of heat transfer was occurring between the ground and the thermosiphon; however, it was the high axial heat transfer potential and the circulation of the refrigerant within the thermosiphon that was most likely responsible for the rapid rebound of the soil around the thermosiphon and the apparent high heat transfer coefficient.

CHAPTER 5

CONCLUSIONS

Although the ground was found to be a more thermodynamically favorable heat source than the ambient air, the vertical U-tube GSHP only attained a COP of about 3 and did not meet the performance expectations suggested in the literature. For heating purposes, and considering the relatively low cost of natural gas, the high installation cost of this particular U-tube GSHP would not be recouped in energy cost savings.

The COP of the thermosiphon was not evaluated, but it was found that the heat transfer rate per unit length associated with the thermosiphon was approximately 2.3 times greater than the heat transfer rate per unit length associated with the U-tube GSHP. The thermosiphon was more effective than the U-tube at supplying heat to the heat pump.

A subterranean heat transfer analysis was also conducted on both the U-tube system and the thermosiphon. Based on the transient temperature response of both systems, a conceptual heat transfer model was developed to analyze the convective heat transfer between the flowing groundwater and the thermal grout. Based on this model, a method was developed and successfully implemented to accurately predict the heat transfer coefficient between the flowing groundwater and the thermal grout sealing the U-tube pipe. With this method, only temperature measurements along the length of the U-tube pipe were necessary to infer the heat transfer coefficient. This method did not require

direct measurement of the groundwater velocity. From normalized logarithmic slope fits, the Biot number for the U-tube system was found to be between 0.25 and 0.45. Considering the thermal conductivity of both the thermal grout and the native soil, it was determined that the Nusselt number for the U-tube system ranged from 0.62 to 1.1. From the experimental Nusselt numbers, the heat transfer coefficient for the U-tube was inferred to be between 8 and 14.4 W/m^2-K. The heat transfer coefficient associated with the U-tube is on the same order of magnitude as air flowing over a cylinder.

To confirm the accuracy of the Nusselt numbers, the groundwater flow velocity was estimated, and using an appropriate correlation, a theoretical Nusselt number was obtained. This theoretical Nusselt number fell within the range of Nusselt numbers found experimentally. This verified the accuracy of the logarithmic slope fit method.

However, the logarithmic slope fit method did not yield accurate results for the thermosiphon. The Biot number for the thermosiphon was found to be between 3 and 4.5. The Nusselt number was found to be between 7.2 and 10.8 resulting in a heat transfer coefficient between 96 and 144 W/m^2-K. This value was 10 times greater than the predicted theoretical result. Upon closer inspection, it was the thermosiphon's high axial heat transfer potential that was most likely responsible for the redistribution of thermal energy and an apparent high heat transfer coefficient. The method for inferring the heat transfer coefficient accurately predicted the heat transfer coefficient of the U-tube GSHP but not for the thermosiphon.

5.1 Recommendations

Several inefficiencies were noted as adversely affecting the performance of the U-tube system. Reducing these inefficiencies could improve the performance of the U-tube system. Digging a wider diameter borehole may allow the supply leg to be moved farther away from the return leg reducing the inadvertent heat transfer that takes place between the two legs. Another way to accomplish this would be to place each leg in a separate borehole. Also, constructing the U-tube out of a more conductive material such as galvanized steel may improve the thermal connection between the U-tube system and the soil. These suggestions incur additional cost to the already expensive installation process, but options such as these should be explored, and studies should be conducted to determine how to improve the efficiency of the U-tube system.

It is important to note that this analysis was only valid for the heating season. Another analysis is necessary to compare the cooling performance of a U-tube system to an air conditioning unit.

More studies can also be conducted to improve or create new methods for inferring the heat transfer coefficient. The logarithmic slope fit method accurately predicted the heat transfer coefficient for the U-tube system, but it did not produce accurate results for the thermosiphon. Also, this method was only proven to be accurate for moderate velocity ground water flow. At high velocity groundwater flow, convection becomes increasingly important. In such cases, a method for inferring the heat transfer coefficient would be extremely useful. Further tests should be done to confirm the accuracy of this method for high-velocity groundwater flow. Also, a method should be developed that takes into account the axial temperature redistribution associated with the thermosiphon.

In future studies, an improved experimental configuration could be implemented. In this experiment, the thermosiphon and the U-tube system could not be operated simultaneously. In future studies that directly compare two or more systems, it is important that those systems be allowed to operate at the same time. This way, the systems can be compared under the same conditions. This can be done by installing the systems in adjacent housing units with similar subterranean conditions. Each housing unit will only operate a single system allowing for an independent comparison. In this way, each system can also be operated for long periods of time without interfering with one another. In this work, the thermosiphon was only operated for approximately eight hours. More accurate data will be obtained if each system is operated independently for longer time periods.

Overall, this study successfully developed and implemented a method for inferring the heat transfer coefficient between moderate-velocity groundwater flow and the thermal grout sealing a U-tube GSHP. This work also found that a U-tube system used only for heating is not very economical compared to traditional systems. Further studies should be conducted to expand the logarithmic slope fit method and to seek improvements for the U-tube system.

REFERENCES

[1] D&R International, Ltd. (2011). *2011 Buildings Energy Data Book* [Online]. U.S. Department of Energy. Available: http://buildingsdatabook.eren.doe.gov/default.aspx [Apr. 1, 2012].

[2] MIT led interdisciplinary panel, "The Future of Geothermal Energy," MIT, Cambridge, Ma, 2006.

[3] G. Florides and S. Kalogirou, "Ground Heat Exchangers--A Review of Systems, Models and Applications," *Renewable Energy*, vol. 32, no. 15, pp. 2461-2478, Dec., 2007.

[4] K. S. Udell et al., "Net Zero Energy Air Conditioning Using Smart Thermosiphon Arrays," 2011 ASHRAE Winter Conference, Las Vegas, NV, *ASHRAE Transactions*, vol. 117, p.892, 2011.

[5] A. Omer, "Ground-Source Heat Pumps Systems and Applications," *Renewable and Sustainable Energy Reviews*, vol. 12, pp. 344-371, 2008.

[6] J. Lund et al, "Geothermal (Ground-Source) Heat Pumps – A World Overview," *Geo-Heat Center Bulletin*, 2004.

[7] S. Kavanaugh et al., "Cost Containment for Ground-Source Heat Pumps," Department of Mechanical Engineering, University of Alabama, Tuscaloosa, AL, 1995.

[8] "Geothermal Heating,"
Internet: http://www.mankysanke.co.uk/html/geothermal_heating.html [Apr. 30, 2012].

[9] P. Dunn and D.A. Reay. *Heat Pipes*, 4th ed. Oxford, England: Pergamon Press, 1994.

[10] International Ground Source Heat Pump Association. (2012). "About Us," IGSHPA [Online]. Oklahoma State University, Stillwater, OK.
Available: http://www.igshpa.okstate.edu/about/about_us.htm

[11] International Ground Source Heat Pump Association, "Lipscomb University Ezell Center Case Study," Oklahoma State University, Stillwater, OK, 2009.

[12] P. Lienau et al., "Ground-Source Heat Pump Case Studies and Utility Programs," Geo-Heat Center, Oregon Institute of Technology, Klamath Falls, OR, 1995.

[13] P. Eskilson, "Thermal Analysis of Heat Extraction Boreholes," Doctoral Thesis, Department of Mathematical Physics, University of Lund, Lund, Sweden, 1987.

[14] J. Spitler et al., "Recent Developments in Ground Source Heat Pump System Design, Modeling and Application," *Proc. of CIBSE/ASHRAE joint conference*, Dublin, Ireland, Session 9a, Paper A28, p.34, 2000.

[15] A. Chiasson et al., "A Preliminary Assessment of the Effects of Ground-Water Flow on Closed-Loop Ground-Source Heat Pump Systems," *ASHRAE Transactions*, vol. 106, pp. 380-393, 2000.

[16] G. Hellström, "Thermal Performance of Borehole Heat Exchangers," The Second Stockton International Geothermal Conference, Pomona, NJ, 1998.

[17] G.L. Morrison et al., "Water-In-Glass Evacuated Tube Solar Water Heaters," School of Mechanical and Manufacturing Engineering, University of New South Wales, Sydney, Australia, 2001.

[18] C.E. Heuer, "The Application of Heat Pipes on the Trans- Alaska Pipeline," Special Report 79-26, Cold Regions Research and Engineering Laboratory, US Army Corps of Engineers, Hanover, NH, 1979.

[19] S. Sorensen et al., "Thermal Performance of TAPS Heat Pipes with Non Condensable Gas Blockage." *Proceedings of the 11th International Conference on Cold Regions Engineering*: *Cold Regions Impacts on Transportation and Infrastructure*. Anchorage, AK, pp.1-12, 2002.

[20], L.L. Vasiliev et al., "Heat Pipes and Heat Pipe Exchangers for Heat Recovery Systems," *Journal of Heat Recovery Systems*, vol. 4, pp. 227-233, 1984.

[21] K. Ochsner, "Carbon Dioxide Heat Pipe in Conjunction with a Ground Source Heat Pump (GSHP)," *Applied Thermal Engineering*, vol. 28, no. 16, pp. 2077-2082, 2008.

[22] K.S. Udell et al., "Seasonal Underground Thermal Energy Storage Using Smart Thermosiphon Technology," *2009 Annual Meeting, Transactions of the Geothermal Resources Council*, Reno, NV, vol. 33, pp. 643-647, 2009.

[23] C. Workman, "Comparison of U-Tube Boreholes and a Thermosiphon on Heat Pump Performance in an Aquifer." MS Thesis, Department of Mechanical Engineering, University of Utah, Salt Lake City, UT, 2011.

[24] S. Nakai and T. Okazaki. "Heat Transfer from a Horizontal Circular Wire at Small Reynolds and Grashof Number – 1 Pure Convection," *Int. Journal Heat Mass Transfer*, vol. 18, pp. 387-396, 1975.